FACULTY OF SCIENCE AND TECHNOLOGY

MASTER THESIS

Study programme / specialisation:
Petroleum Technology /Reservoir Engineering

The spring semester, 2022

Open / Confidential

Author: Saja H. A. Algazban

.....
(signature author)

Course coordinator: Øystein Arild

Supervisor(s):
Skule Strand
Tina Puntervold
Ivan Dario Pinerez Torrijos

Thesis title: Polysulphate as Smart Water Additive for Improved Oil Recovery from Carbonate Reservoirs

Credits (ECTS): 30

Keywords:

Enhanced Oil Recovery

Polysulphate

Spontaneous Imbibition

Wettability Alteration

Pages: 89

+ appendix: 9

Stavanger, 15/2022
date/year

Abstract

The potential of improving the oil recovery in carbonates is very high due to a combination of significantly high amount of hydrocarbon that is held within carbonate reservoirs and a low oil recovery. Since most carbonates are neutral to slightly oil wet, altering the wettability towards more water wet conditions by injecting a low-cost water based EOR brine called Smart Water has been a great success.

Smart Water has a specific ionic composition that increases the water-wetness of the reservoir, which induces favourable capillary forces and an increase the microscopic sweep efficiency. A Smart Water that has been an excellent success in Ekofisk chalk reservoir is seawater (SW). SW has shown a great EOR effect as it modifies the wettability towards more water-wet state due to containing the three potential determining ions Mg^{2+}, Ca^{2+} and SO_4^{2-}.

In this thesis, the use of the natural occurring polysulphate (PS) salt ($K_2Ca_2Mg(SO_4)_4 \cdot 2H_2O$) as an additive to improve the oil recovery in chalk cores is investigated. Since PS contains the three determining ions that are crucial for wettability alteration it has the potential of being a wettability modifier. To further evaluate the wettability alteration of PS it was used as an additive in distilled water (DW), with no active ions, and SW, a well-known Smart Water with active ions. To evaluate the wettability alteration, spontaneous imbibition test was used as the quantitative method.

Stevns Klint (SK) chalk cores were used to resemble a North Sea reservoir chalk condition. The outcrop cores were restored with 10% initial formation water and were 90 % oil saturated, all cores were aged for 2 weeks, spontaneous imbibition was the main tests to evaluate the core's wettability, the cores were imbibed with different brines at both 90 and 110° C, being these, formation water (FW), SW, SW-PS, DW-PS.

The use of PS salt in both SW and DW provided brines with Smart Water composition, holding adequate proportion of the three potential determining ions Mg^{2+}, Ca^{2+} and SO_4^{2-}. DW-PS and SW-PS confirmed inducing wettability alteration as the %OOIP was significantly higher than imbibing FW with 35.2% and 44.8% recovered oil at 90 and 110 °C respectively, with an increase of 13.4% and 23.0% recovered oil respectively, compared to FW.

The performance of DW-PS at both 110°C and 90°C was slightly lower than SW with 1 to 2% difference in oil recovery. This provides an opportunity to obtain the same outstanding results on onshore fields where there is no or limited access to SW. The PHREEQC simulation showed consistency with the experimental results and stability of the composition.

Acknowledgements

I would like to express my sincere gratitude for associate professors Tina Puntervold and Skule Strand for the opportunity of letting me be a part of the EOR team by giving me an interesting and challenging topic. Thank you for valuable and informative discussions regarding this research. This research has increased my knowledge of EOR a significantly by combining both theoretical and practical work

I am also very grateful of Dr. Iván Darió Piñerez Torrijos for his guidance, help, and support throughout this research. The discussions we had, for both the theoretical part and the practical part of this thesis, was very valuable for further understanding. I would also like to thank Phd student Md Ashraful Khan for the guidance and knowledge in the laboratory. Without him, I would not be independent in my laboratory work.

A special thanks to my co-student Sander Haaland Kleiberg for the collaboration on oil preparation and core restoration. Your help is of great value. I would also like to extend my appreciation to my lab partners Mahmood Fani and Giannis Kalampalikis for an unforgettable and fun work environment.

Finally, I would like to thank my family, friends and my dear husband, Mohammed Al-Omari for being very supportive and encouraging through this research.

Saja H. A. Algazban

15th of June 2022

Table of Contents

List of Figures

List of Tables

Nomenclature

AN	Acid number
BN	Base number
D	Core diameter
DI-water	Deionized water
DW	Distilled water
DW-PS	Distilled water Polysulphate
E	Overall displacement efficiency
E_D	Microscopic displacement efficiency
EOR	Enhanced oil recovery
E_V	Macroscopic displacement efficiency
FVF	Formation volume factor
FW	Formation water
IFT	Interfacial tension
IOR	Improved oil recovery
IOIP	Initial oil in place
k	Permeability
L	Core length
M	Mobility ratio
NF	Nanofiltration
N_p	Oil displaced
OOIP	Original oil in place
P_c	Capillary pressure
PS	Polysulphate
PV	Pore volume
SI	Spontaneous Imbibition
S_{or}	Residual oil saturation
SW	Seawater
S_{wi}	Initial water saturation
SW0NaCl	Seawater zero sodium chloride
SW-PS	Seawater Polysulphate

USBM	United States Bureau of Mines
V_b	Bulk volume

1. Introduction

Carbonate reservoirs make up to 50% of the reservoirs worldwide where it holds more than 60% of the oil and 40% gas of the world's oil and gas reserves (Bjørlykke, 2015; Schlumberger). Even though it holds a significant amount of hydrocarbons reserves, the oil recovered from these reservoirs is less than 30% of IOIP. This is far less than what is obtained from sandstone reservoirs making the enhanced oil recovery (EOR) potential of carbonates very high (Austad et al., 2008; Hognesen et al., 2005).

Carbonates are known for having properties that are not favourable for oil recovery. Around 90% of the carbonate reservoirs are neutral to oil-wet with a small to negative capillary pressure that prevents the water from imbibing spontaneously into the rock matrix. Combining this with a permeability in the range of 1-10 mD and natural occurring fractures, the oil produced will be displaced from the high permeable fractures rather from the pores resulting in early water breakthrough. With a porosity of up to 50 %, the oil recovered by water flooding has been very low.

Since the wetting property is dynamic, it has been a great focus on finding a method that alter the wetting condition towards being more favourable for oil recovery. A method of using expensive cationic surfactants of the type $R - N(CH_3)_3{}^+$ has been suggested (Hognesen et al., 2005). Another method shows that heating the matrix block by steam or water injection induces wettability alteration by rendering the matrix water-wet (Al-Hadhrami and Blunt, 2001). The most successful method of altering the wettability has been the use of ''Smart Water'' brines; brines with a specific ionic composition (Fathi et al., 2011).

A well-known Smart Water fluid in carbonate reservoirs is seawater (SW). SW has been an excellent success in the Norwegian continental shelf with an oil recovery approaching 50%. This enhancement is a result of wettability alteration in the porous media from mixed-wet towards more water-wet. The drive behind this mechanism is a symbiotic interaction between the active cations calcium (Ca^{2+}), magnesium (Mg^{2+}), and sulfate (SO_4^{2-}) in SW, and the mixed-wet calcite ($CaCO_3$) surface. (Austad et al., 2007). Furthermore, it has also been confirmed by a study performed by Zhang and Austad, (2006) that SO_4^{2-} acts as a catalyst for the wettability alteration process. The EOR potential by spontaneous imbibition at low

temperature, 70°C, was verified to be increased by spiking SW with SO_4^{2-} with an oil recovery above 50%, see Figure 1a (Zhang and Austad, 2006). Same experiment was performed at high temperature, 100°C, shows that the oil recovery almost doubled by using SW spiked 4 times the SO_4^{2-}- concentration of SW. Even though the effect is favourable, spiking SW with SO_4^{2-} is not recommended at high temperatures as it leads to precipitation of anhydrite, $CaSO_4$ (s) (Zhang and Austad, 2006; Zhang et al., 2007).

Recently studies have also shown that some certain modification of the ionic composition in SW improves the oil recovery even further. A study performed by Fathi et al., 2011, shows how eliminating $NaCl$ from SW, termed as SW0NaCl in Figure 1b, increases the oil recovery by spontaneous imbibition that is beyond that of SW with $NaCl$. By taking the same brine, SW0NaCl, and spiking it with $SO_4^{2-}$the oil recovery gets significantly higher with more than 20% oil recovered compared to SW (Fathi et al., 2011).

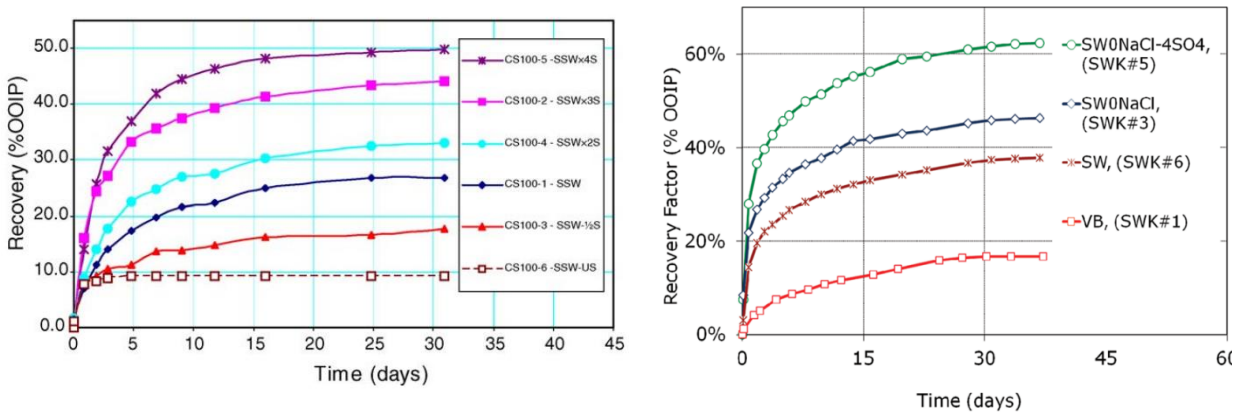

(a) (b)

Figure 1: (a): Spontaneous imbibition at 70 °C showing the EOR effect on chalk cores by spiking SW with SO_4^{2-} (Zhang et al., 2007). (a): EOR effect obtained by spontaneous imbibition at 90 °C on chalk cores by using SW, VB (formation water), and two modified SW brines; SW0NaCl and SW0NaCl-4SO4 (Fathi et al., 2011).

To produce optimized SW is technically possible by combining nano-filtration and reversed osmosis. However, including these two methods to the operation increase the capital investment and operating cost (Ayirala and Yousef, 2014). Moreover, increasing sulphate concentration in the injection brine at high temperature reservoirs might induce scaling problem. Therefore, there is a need for an injection water that is cheap to prepare, stable at high temperatures, and work as effective as or better than smart water, which for carbonate reservoirs is SW, by increasing the oil recovery.

1.1. Objective

The main objective of this thesis is to investigate the EOR effect of a salt called polysulphate (PS) as an EOR additive in both SW and freshwater, PS is derived from polyhalite and with the chemical formula $K_2Ca_2Mg(SO_4)_4 \cdot 2H_2O$ it has the potential of being a smart water as it contains the three determining ions (Ca^{2+}), (Mg^{2+}), and (SO_4^{2-}). SO_4^{2-} acts as a catalyst in wettability alteration process by adsorbing onto the positively charged chalk surface.

The secondary objectives of this thesis are:

- Two PS brines will be evaluated. PS in SW and PS in freshwater. The quantitative results will then be compared with SW and FW, where FW is used as the reference without wettability alteration taking place, and SW is a reference for a standard injection brine offshore.

- Temperature effects will be investigated by preforming spontaneous imbibition test at 70 °C and 110 °C and the efficiency of PS-DW and PS-SW for displacing crude oil from chalk cores will be evaluated.

- To characterize the rock-brine-oil interactions under the presence of PS salt.

- To evaluate the stability of these brines under experimental conditions will be tested and simulations with the geochemical simulator PHREEQC will be integrated in this study.

2. Theory

2.1. Oil Recovery

For conventional oil reservoirs, the operation of oil recovery is traditionally divided into three stages: primary, secondary, and tertiary recovery. These stages describe the production of the reservoir mainly in a chronological order. Depending on the reservoir characteristics, this order can be altered, and stages can be skipped if the crude oil is not produced at flow rates that are economically feasible, e.g. heavy oil (Green and Willhite, 2018).

2.1.1. Primary Recovery

Primary recovery is the first production stage taking place in the reservoir where the production is driven from natural forces such as water drive, gas cap drive, rock and fluid expansion, and gravity drainage (Green and Willhite, 2018). Up to 50% and an average of 19 % of the originally oil in place (OOIP) can be recovered. Primary recovery is usually not enough for extracting, as most of the oil is remained untouched in the reservoir. Thus, a second recovery process needs to be introduced to increase the oil recovery in the reservoir (Alamooti and Malekabadi, 2018).

2.1.2. Secondary Recovery

The secondary recovery process is implemented once the driven natural forces from the first stage reduce, or the process is inefficient to begin with and yields an overall low recovery. In secondary recovery, artificial drive is introduced to the reservoir supplementing the natural forces. The most common method is water injection, but gas injection is also used.

Water injection is conducted to give pressure support to the reservoir and to displace the oil towards producing wells. Gas injection in this stage is injected either into gas cap for pressure support or to displace oil immiscibly by injecting into an oil-column well. All other gas processes based on other mechanisms are considered to be EOR processes, such as oil swelling, oil viscosity reduction, or favourable phase

behaviour (Green and Willhite, 2018). Since water injection is more effective and an energy-saving method than gas injection, it is considered to be equivalent to secondary recovery (Alamooti and Malekabadi, 2018).

2.1.3. Tertiary Recovery - Enhanced Oil Recovery

After implementing primary and secondary recovery processes, all the irrecoverable oil is then extracted by conducting methods that do not involve natural forces nor water/gas injection. These methods are considered as tertiary recovery processes. Since primary or both primary and secondary recovery are bypassed in some cases due to ineffectiveness and/or economical insufficiency, the term ‘’tertiary recovery’’ became unfavourable as it is not always representing the third recovery stage. Therefore, this process is referred to as enhanced oil recovery (EOR) as this term is chronological independent.

In EOR process, fluids chemicals or gases that are not initially in the reservoir is injected to interact with the reservoir rock, oil, and water. This interaction may lead to lower interfacial tension (IFT), lower oil viscosity, oil swelling and wettability alteration which then alter the initial condition of the system to be more favourable for oil recovery (Green and Willhite, 2018).

2.2. Wettability

An important term that plays a major role in EOR is wettability. Wettability is defined by (Craig, 1971) as ‘’*the tendency of one fluid to spread on or adhere to a solid surface in the presence of other immiscible fluids’’*. In a multiphase reservoir, the microscopic phase distribution within the rock pores is determined by the wettability of the rock, which is the preference of one liquid phase to be in contact with the rock surface in the porous medium in presence of the other liquid phase (Craig, 1971). There are four type of wettability states in a water/oil/rock system: water-wet, fractional-wet, mixed-wet, and oil-wet.

Water-wet System

When more than 50% of the rock surface is wet by water, the water/oil/rock system is considered to be water-wet, Figure 2. In this system the small pores will be filled by water whereas in big pores the water will act like a film where it covers the rock surface. The oil, which is the nonwetting phase, will be found in the big pores as droplets laying on the water film. These oil droplets may also extend through two or more pores and even be in contact with the rock surface at areas that contain preferentially oil-wet minerals. Low water saturation, saturation near or at initial water saturation, S_{wi}, gives us a system where the wetting phase (water) remains continuous in the small pores whereas the nonwetting phase is continuous in the larger pores. By increasing the water saturation, the oil in the larger pores becomes discontinuous and will eventually be surrounded by water.

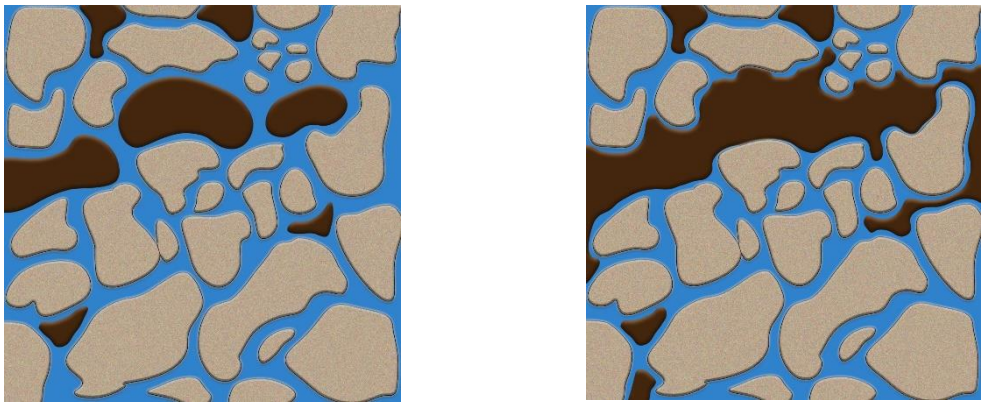

(a) (b)

Figure 2: Illustration of water-wet system where (a) shows the system at a water saturation greater than S_{wi} and (b) reflects a system near or at S_{wi}. Figures were drawn after description by Donaldson and Alam (2008)

:

If an oil saturated system that is preferentially water-wet gets in contact with water, the water will spontaneously imbibe the system by displacing the oil until reaching static equilibrium between the capillary forces of the fluids and the rocks surface energy force. Taking the same system, but initially water saturated, the oil will not be capable to imbibe the system (Donaldson and Alam, 2008).

Fractional-wet System

The term fractional wetting is used to describe a heterogeneous wetting of the rock surfaces in the pores, see illustration in Figure 3. The preferential wetting of the rock is randomly distributed due to random distribution of minerals that can either prefer to be water- or oil-wet. Since these minerals are scattered, it will be difficult for the oil to have a continuous contact with the rock surface in larger pores compared to a water-wet system where the oil form a continuous network (Donaldson and Alam, 2008).

Figure 3: Fractional-wet system where the preferential wetting are heterogeneous. Drawn after description by Donaldson and Alam (2008)

Mixed-wet System

In a mixed-wet water/oil/rock system, the small pores will be fully saturated with water as well in contact with the rock surface and the larger pores will be oil-wet and fully saturated with oil, see illustration in Figure 4. In this case, the oil will form a continuous network throughout the rock. This mixed-wet system has probably established during the original accumulation of oil where the surface of the rock contains oil active compounds that displace the connate water. The water film that remains on the pore surface will gradually be displaced leaving the oil as the only wetting fluid. Since the capillary pressure threshold for displacing water in the small pores is too large, the oil will not enter these pores (Donaldson and Alam, 2008).

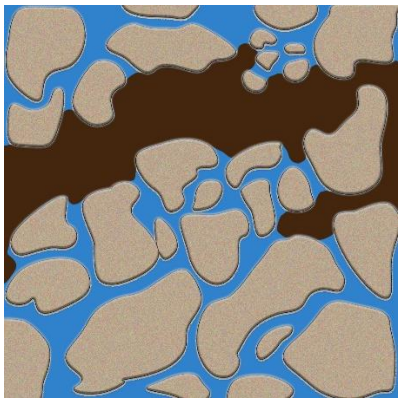

Figure 4: Mixed-wet system where the big pores are fully saturated and in contact with oil and the small pores are fully saturated and in contact with water . Drawn after description by Donaldson and Alam (2008)

Oil-wet System

The oil-wet system is the opposite of a water-wet system where the small pores is saturated with oil and the surface of the larger pores is in contact with the oil, Figure 5. When the system has higher water saturation and is near the residual oil saturation (S_{or}), the water droplets will connect and make a continuous network in the larger pores. The same behaviour occurs in water-wet system but with oil as the connecting phase. As the system gets higher oil saturation, the continuous water network will poorer due to the oil covering the rock surface area in the larger pores creating oil film and leading the water to be centred in the pore. In this case, the water is the nonwetting phase whereas the oil is the wetting phase (Donaldson and Alam, 2008).

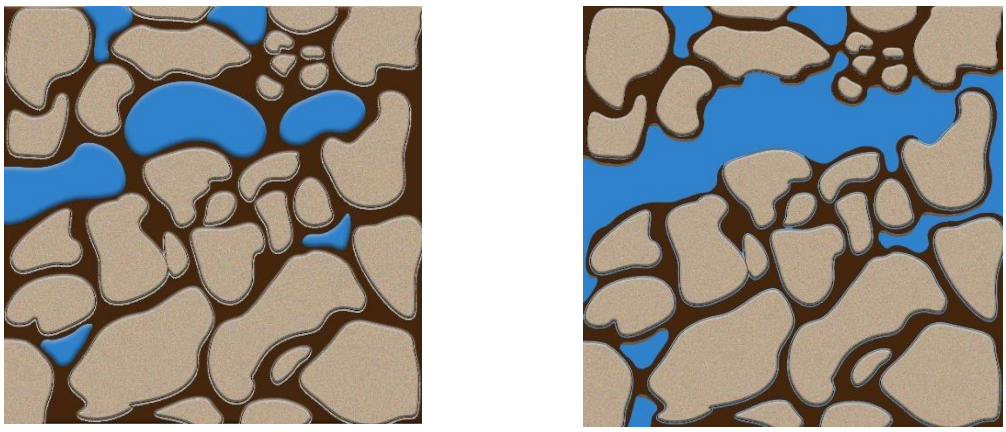

(a) (b)

Figure 5: Oil wet system where (a) shows the system at an oil saturation greater than S_{or} and (b) a system near or at S_{or}. Drawn after description by Donaldson and Alam (2008)

2.3. Displacement Efficiency

The recovered oil, in fraction, that was initially in place at start of an EOR process corresponds to the overall displacement efficiency, E, that consist of microscopic displacement efficiency, E_D, and macroscopic displacement efficiency, E_V. The efficiency of the overall displacement can be quantified by the product of microscopic and macroscopic displacement efficiency as follows:

$$E = E_D E_V \tag{2.1}$$

Microscopic displacement is the displacement of oil when contacted by the displacing fluid at the pore scale. E_D measures how effective the displacing fluid is to mobilize the contacted oil that is trapped in the pores. After the displacing fluid has been swept through the pore medium, the oil remaining in the pores is the residual oil. Therefore S_{or} is an essential part that determines how efficient is the microscopic displacement:

$$E_D = \frac{S_{oi} - S_{or}}{S_{oi}} \tag{2.2}$$

Macroscopic displacement describes the displacement of oil from the pore volume of the reservoir. When injecting the displacing fluid into the reservoir, large sections of the reservoir remain untouched by the injecting fluid. The less reservoir volume the injecting fluid contacts the lower the macroscopic displacement efficiency gets and thus lower E.

E_V can be expressed by using the material-balance concepts by assuming a piston-like oil displacement of the process. If a displacement process reduces the oil from initial to residual saturation in the contacted regions, the oil displaced can be calculated as follows:

$$N_p = \left(\frac{S_{o1}}{B_{o1}} - \frac{S_{o2}}{B_{o2}}\right) V_p E_v \tag{2.3}$$

Where,

N_p	oil displaced and produced by the displacing fluid
S_{o1}	initial oil saturation at the beginning of the process
S_{o2}	residual oil saturation in the contacted reservoir regions at the end of the process
B_{o1}	formation volume fraction (FVF) at the beginning of the process
B_{o2}	FVF at the end of the process
V_p	pore volume, PV, of the reservoir.

Rearranging equation 1.3 with respect to E_v:

$$E_v = \frac{N_p}{V_p\left(\frac{S_{o1}}{B_{o1}} - \frac{S_{o2}}{B_{o2}}\right)} \tag{2.4}$$

For an ideal EOR process, it is desirable that both E_D and E_V approach 1.0. For this case the total reservoir volume will be contacted by the displacing fluid to mobilize and displace the oil towards production wells. In addition, all oil will be removed from the pores making the S_{or} approach 0 (Green and Willhite, 2018).

2.3.1. Fluid Flow Through Porous Media

Fluid flow through the porous media is an important aspect in EOR as it increases our understanding of how the various fluids flow and interacts with each other. An important property in an unfractured reservoir is the permeability. Permeability tells us how well the pores are connected. For a low permeable reservoir, the oil will flow poorly and even be trapped within the porous media (Atangana, 2018; Green and Willhite, 2018). Henry Darcy (1856) derived an expression known as the Darcy's law that describes the flow of oil and water in the reservoir:

$$q = -\frac{k \cdot A}{\mu}\frac{\Delta P}{L} \tag{2.5}$$

Where,

q volumetric flow rate (m^3/s)

k permeability (mD)

A cross-sectional area (m^2)

μ fluid viscosity (Pa·s)

ΔP differential pressure (Pa)

L core length (m)

In a multiphase reservoir the permeability determined from Darcy's equation is the relative permeability, the ratio of effective permeability of a certain fluid to the absolute permeability of the same fluid, where the effective permeability is the fluid ability to flow in presence of other immiscible fluids and absolute permeability is the fluid ability to flow when only one phase is present in the porous media (Schlumberger). Another important term in EOR is mobility and mobility ratio. In a multiphase reservoir, mobility is defined as the ratio of effective permeability to phase viscosity. For a single-phase reservoir, absolute permeability is used. Mobility can be formulated as follows:

$$\lambda = \frac{k_e}{\mu} \tag{2.6}$$

Where,

λ mobility (m^2/ Pa·s)

k_e effective permeability (mD)

μ fluid viscosity (Pa·s)

When displacement processes are involved, mobility ratio (M) will be of great importance as it affect both areal and vertical displacement. In an ideal displacement process water should be displacing oil from behind creating a piston-like displacement. This favourable displacement occurs only when M is less than 1.0. For unfavourable displacement, M will be greater than 1.0 creating a phenomenon called viscous fingering (Green and Willhite, 2018). Assuming a piston-like displacement during waterflooding, the mobility ratio is given as follows:

$$M = \frac{\lambda_D}{\lambda_d} = \frac{\left(\frac{k_{rw}}{\mu_w}\right)_{S_{or}}}{\left(\frac{k_{ro}}{\mu_o}\right)_{S_{wi}}} \tag{2.7}$$

Where,

M	mobility ration (dimensionless)
λ_D	mobility of the displacing fluid (m^2/ Pa·s)
λ_d	mobility of displaced fluid (m^2/ at residual oil saturation)
$(k_{rw})_{S_{or}}$	relative permeability of water at residual oil saturation (m^2)
$(k_{ro})_{S_{wi}}$	relative permeability of oil at initial water saturation (m^2)
$(\mu_w)_{S_{or}}$	water viscosity at residual oil saturation (Pa·s)
$(\mu_o)_{S_{wi}}$	oil viscosity at initial water saturation (Pa·s)

2.4. Displacement Forces

Immiscible displacement of oil through the porous medium involves various forces acting on both oil and the immiscible fluid. The forces that play a significant role in oil mobility and thus the oil production are viscous forces, gravity forces and capillary forces (Morrow, 1979). Oil is usually displaced and produced by two processes; spontaneous imbibition that is influenced by capillary and gravity forces and forced imbibition which is the driven by viscous forces. In forced imbibition, viscous forces need to overcome capillary forces to mobilize and sweep the oil (Green and Willhite, 2018).

2.4.1. Viscous Forces

When a fluid flows through the porous media it will resist the shearing motions that occurs due to the movement of the fluid. This resistance to shearing motions is defined as the viscous force of the fluid (Arfken et al., 1984). The porous medium can be considered as a bundle of parallel capillary tubes with equal length and diameter. Given this assumption, the viscous forces of the fluid will result in a

pressure drop across the capillary tube (Green and Willhite, 2018). For laminar flow the pressure drop can be described by Poiseuille's law:

$$\Delta p = -\frac{8\mu L\bar{v}}{r^2 g_c} \tag{2.8}$$

Where,

Δp pressure drop

μ viscosity of the fluid

L length of the tube

$\bar{v}$ average velocity

r radius of the tube

g_c conversion factor

2.4.2. Gravity Forces

Gravity force has an impact on a multiphase reservoir during production, especially in an oil/gas system where the density of these two fluids differs significantly. The effect of gravity force is especially perceptible in tilted reservoirs where the oil is moved or drained downwards whereas the gas moves upwards resulting in a segregation between these two phases. This gives us an oil production with low gas-oil ratio and a gas cap with a stable high oil saturation (Hall, 1961). Gravity forces has also been reported by (Austad and Milter, 1997) to be the dominating force during oil production at low IFT and that an increase in the height of the permeable rock matrix gives an increase in gravity forces. The hydrostatic pressure that occurs between oil and water due to gravity is given by:

$$\Delta P_g = \Delta \rho g h \tag{2.9}$$

Where,

ΔP_g	hydrostatic pressure between oil and water due to gravity (Pa)
$\Delta\rho$	density difference between oil and water $(\rho_w - \rho_o)$ (kg/m^3)
g	gravitational acceleration constant, 9.81 (m/s^2)
h	height of fluid column (m)

2.4.3. Interfacial Tension

Interfacial tension is a surface energy that occurs when two immiscible fluids such as liquid-liquid or gas-liquid are in contact with each other and separated by a few molecular diameters thick interface. This interfacial tension will likely appear as a membrane which consist of molecules in tension. The force acting at the interface is directed inwards towards the centre to create a sphere that minimizes the surface while the force that is within the liquid is applied in all direction from the attracted molecules, see Figure 6. The tension that occurs at the interfaces between liquid-liquid, gas-liquid, liquid-solid and gas-solid is defined as the surface free energy per unit area (Donaldson and Alam, 2008).

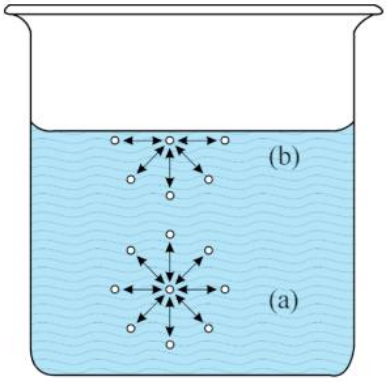

Figure 6: Illustration of how the attractive molecular forces interact with each other in the bilk liquid (a) and at the surface (b)

If a capillary tube is inserted in a container with two immiscible fluids let say water and oil, a thin film of molecules from the wetting liquid, water, will be adsorbed on to the capillary walls making the surface area high. To reduce the total surface area, the water that wet the walls rises in the tube resulting in reduction of the total surface area. When a liquid is not adsorbed on to the capillary walls it will be depressed

forming a convex curve. This behaviour occurs due to a higher mutual attraction of the liquid's molecules than the molecular attraction of the glass-liquid. Since the depressed nonwetting liquid is located at a distance, h, below the liquid level outside the capillary it has a higher pressure, P_2, than the pressure, P_1, just above the interface in capillary tube, see Figure 7.

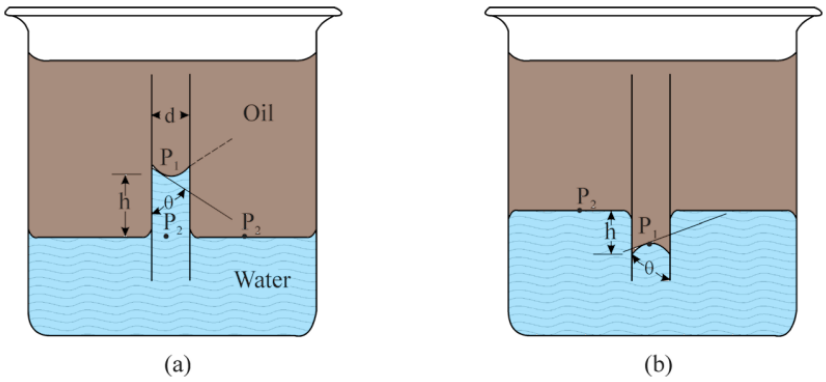

Figure 7: (a) Capillary rise due to adsorbtion of the wetting liquid, water, and (b) depression of the nonwetting fluid, water.

2.4.4. Capillary forces

Forces that occur when a fluid rises in a capillary tube by the influence of wettability is called capillary forces (Donaldson and Alam, 2008). Capillary forces along with interfacial forces are important parameters in EOR processes as it influences the amount of oil trapped in the porous media, especially in unfractured reservoirs where the only pathway for oil is the pore throats. To mobilize the residual oil in the reservoir, capillary forces must be reduced due to a reduction in IFT or by being overcome by other forces. In spontaneous imbibition process the driven forces for displacing and recovering oil is mostly capillary forces but gravity forces might as well influence the recovery. Capillary forces can be overcome and induce flow in the porous system by overcoming the capillary pressure (Green and Willhite, 2018).

Capillary Pressure

Capillary pressure is defined as the pressure difference across the interface. The interface between two immiscible fluids tends to curve due to capillary forces in tight spaces, such as in a small tube, a burette, or in the pore throat in the porous media. On the convex side of the curve, the pressure difference across the interface is greater. This balances the forces that creates the interfacial tension (Donaldson and Alam, 2008). Capillary pressure can be calculated as follows:

$$P_c = P_{nw} - P_w = \sigma\left(\frac{1}{r_1} - \frac{1}{r_2}\right) = \frac{2\sigma Cos\theta}{r_t} \tag{2.10}$$

Where,

P_{nw} nonwetting fluid pressure

P_w pressure of the wetting fluid

r_1, r_2 radii of the curvature of interface

r_t radius of the capillary tube

There are two processes describing the displacement driven by capillary forces: *drainage* and *imbibition.* In a drainage process the nonwetting phase, let say oil, displaces the wetting phase, water, in the porous medium. The opposite process is imbibition where water displaces the oil. To understand whether the porous system undergoes an imbibition or a drainage process, it is important to know the wetting properties of the rock matrix. If the rock is preferentially water-wet the imbibing fluid is water. For preferentially oil-wet rock the imbibing fluid is oil. If the rock is mixed-wet both water and oil can be the imbibing fluid. To avoid any confusion regarding these two terms, the best way to describe the displacement process is by referring to the fluid leaving the core as the *displaced fluid* and the fluid entering the core as the *injected fluid*. For spontaneous imbibition process the term *imbibing fluid* will be used rather than injected fluid (Donaldson and Alam, 2008).

2.5. Wettability Measurement

Since wettability is an important key parameter that controls the residual oil saturation in the porous media, especially in EOR processes, it is by great interest to measure and quantify this parameter. Several methods have been proposed as a way of measuring wettability. This section will describe the most common methods used to measure wettability. The methods used in this thesis to determine wettability is chromatographic wettability test and spontaneous imbibition.

2.5.1. Contact Angle Measurement

To determine whether the rock surface is preferentially oil or water wet, the wettability of the rock surface needs to be measured. This can be achieved by studying the contact angle, θ_c, between a rock surface and a single water droplet, see Figure 8. The range of the contact angle is ranging from 0 to 180°, where 0° is strongly water-wet and 180° is strongly oil-wet.

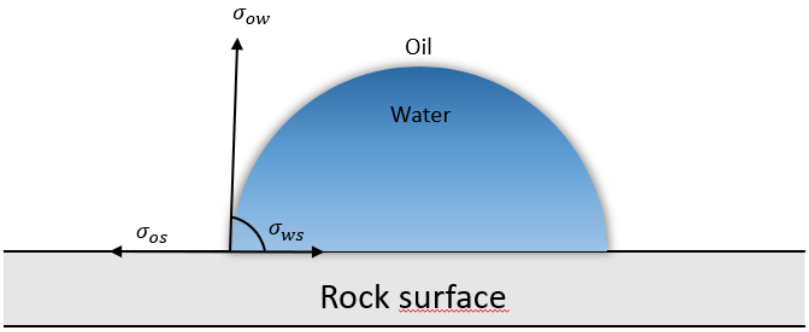

Figure 8: Illustration of contact angle measurement between a rock surface and a water droplet. Redrawn after (Green and Willhite, 2018)

To get a correct measurement of the contact angle, the rock surface must be horizontal and immersed with oil when the water droplet is placed to rest on its surface. If the water is spreading on the surface resulting in a contact angle less than 90°, the rock surface is considered to be preferentially water wet or hydrophilic (strong affinity for water) where the capillary pressure, P_c, is positive. If the water forms a round droplet

on the surface where the contact angle is above 90°, the rock surface is oil-wet or hydrophobic (poor water affinity) and P_c is negative. Getting a contact angle near 90°, indicates a neutral wetting condition with P_c = 0 (Craig, 1971).

The surface tensions that occur in the water/oil/rock systems described above is related to Young-Dupre equation given below:

$$\sigma_{os} - \sigma_{ws} = \sigma_{ow} cos\theta_c \tag{2.11}$$

Where,

σ_{os} = interfacial tension between oil and solid, dynes/cm

σ_{ws} = interfacial tension between water and solid, dynes/cm

σ_{ow} = interfacial tension between oil and solid, dynes/cm

θ_c = contact angle, degree

Contact angle measurement is the most optimal way of measuring wettability on a flat homogenous surface as the only interaction will be between the rock surface and the fluid droplet. The possibility of having surfactants or other compounds altering the wettability is very low. However, the methods of measuring contact angle are complex and are not always suitable for reservoir cores and fluids due to the property of the fluids of adsorbing and desorbing surfactants. In addition, the presence of surface active agents in crude oil makes it time consuming for the contact angle to reach equilibrium (Anderson, 1986).

2.5.2. Spontaneous Imbibition

The phenomenon of a wetting fluid being drawn into a porous media by capillary action is known as spontaneous imbibition (SI) (Morrow and Mason, 2001) . Spontaneous imbibition method is a simple method used to quantify the wettability of a core (Anderson, 1986). In fractured reservoirs with low permeability, oil recovery is mainly influenced by the brine being spontaneously imbibed into the rock. The recovery of oil by SI is dependent on the interaction between oil, water, and rock, which again depends on the wettability conditions and two-phase flow that is determined by the complexity of the chemistry and physical properties of all three

components. On top of that, the fractures and pore structure of the rock do also have an impact on oil recovery.

In a SI experiment, imbibition rate is measured. The method is conducted by saturating the core with oil before placing it in a cell where it has free access to brine. The recovered oil vs time is then used to present the result as the fractional recovery of OIIP vs time (Morrow and Mason, 2001). This information is used to describe the wettability of the core. If the test is performed at reservoir temperatures, the uncertainties related to the physical properties of brine and oil, and temperature effects of core wettability will be reduced (Piñerez et al., 2020).

A modified Amott water index proposed by Pinerez et al., (2020) made it possible to measure the degree of wettability quantitatively rather than qualitatively by still using spontaneous imbibition method. A new modified Amott water index (I^*_{W-SI}) used where the system is strongly water-wet when I^*_{W-SI} = 1 and neutral wet when I^*_{W-SI} = 0. The index is expressed as follows:

$$I^*_{W-SI} = \frac{SI_C}{SI_{WWC}}$$

Where,

I^*_{W-SI}	modified Amott water index
SI_C	oil recovery (%OOIP) by spontaneous imbibition with evaluated wetting state of the core
SI_{WWC}	oil recovery (%OOIP) by spontaneous imbibition in a strongly water-wet reference core

2.5.3. Amott and Amott-Harvey Method

The Amott method (Amott, 1959) is one of the first methods proposed for determining wettability. The Amott method combines the results from both spontaneous imbibition and forced displacement to quantify the average wettability of a core. The method is based on the displacement that occurs when the cores preferred wetting fluid spontaneously imbibe into the core and displace the non-wetting fluid. To reduce the effect of relative permeability, viscosity and initial saturation of the core, the ratio of oil displaced in spontaneous imbibition to the oil displaced in forced imbibition is used (Anderson, 1986).

.

The spontaneous imbibition is performed by placing the saturated core in a cell known as the Amott cell, see illustration in Figure 9. For forced displacement the method is performed by centrifuging the oil saturated core with brine until reaching S_{or}. A modification of the method, known as the Amott-Harvey method, gave an additional preparation step where the core was first centrifuged under brine then under oil before performing the test. This allows the core to reach the initial water saturation (McPhee et al., 2015).

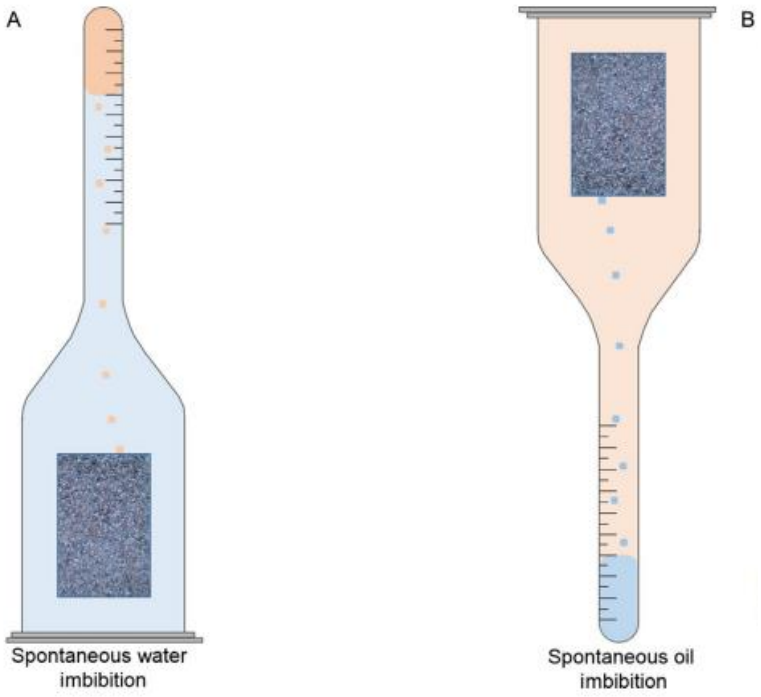

Figure 9: Illustration of the Amott cell used for spontaneous imbibition of (a) water and (b) oil

After preforming the Amott test, wettability indexes, I_w and I_o, for water and oil, respectively, are determined. I_w is obtained by spontaneous imbibition where the core at S_{wi} is immersed in water allowing it to spontaneously imbibibe and displace the oil out of the core. The change of water saturation, ΔS_{ws}, in the core is recorded. After reaching the maximun oil recovery, forced displacement, ususally by centrifuging, is then performed to increase the water saturation of the core even further. The change of water saturation by forced dispacement is termed as ΔS_{wf} (Morrow, 1990). The I_w can then be formulated as follows:

$$I_w = \frac{\Delta S_{ws}}{\Delta S_{ws} + \Delta S_{wf}} \tag{2.12}$$

If the only change in water saturation occurs during spontaneous imbibition. The core is more likely to be preferentially water-wet and the I_w will be close to or equal to 1. For I_o, the oil is spontaneously imbibed (drainage) displacing the water out of the core before preforming forced imbibition of water by oil. Similarly, I_o will be close

to or equal to 1 if the core is preferentially oil-wet where the change of oil saturation, ΔS_{os} ,only occurs during spontaneous imbibition. Change of oil saturation as a result of forced imbibition is termed ΔS_{os}. I_o is then expressed as:

$$I_o = \frac{\Delta S_{os}}{\Delta S_{os} + \Delta S_{of}} \tag{2.13}$$

Combining these two Amott indices by subtracting I_w from I_o gives us the Amott-Harvey index, I_{AH}, expressed as one single number:

$$I_{AH} = I_w - I_o \tag{2.14}$$

The Amott-Harvey index varies from +1, indicating complete water-wet system, to -1, a complete oil-wet system. The system can be characterized as slightly water wet when the value of I_{AH} ranges from +0.1 to +0.3, neutral wet in the range of +0.1 to -0.1 and slightly oil-wet in the range -0.3 to -0.1 (Cuiec, 1984). A complete Amott-Harvey test, Figure 10, consist of the following 5 different stages (Anderson, 1986):

1. Establishment of S_{wi} by forced displacement (oil displacing water)
2. Spontaneous imbibition of water
3. Forced imbibition of water
4. Spontaneous imbibition of oil (drainage)
5. Forced displacement of oil (drainage)

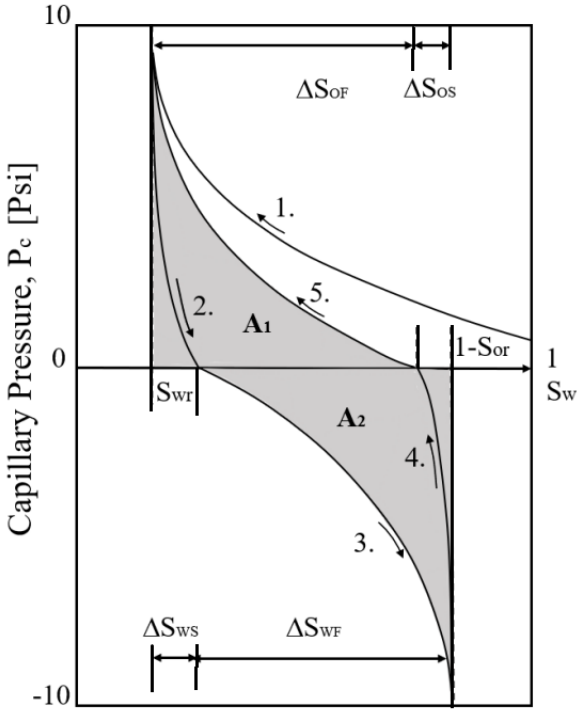

Figure 10: Capillary curve vs saturation for Amott and Amott-Harvey wettability test method. Redrawn after Tina Puntervold (2008)

In an Amott test, forced displacement can also be performed by using a sample core holder instead of a centrifuge but since the data collected from the centrifuge can be used to determine the wettability in United States Bureau of Mines method, the use of centrifuge is more preferred (McPhee et al., 2015).

2.5.4. United States Bureau of Mines (USBM)

Another quantitative method, developed by (Donaldson et al., 1969), of measuring the wettability is the United States Bureau of Mines (USBM). This method uses the capillary pressure curves, illustrated in Figure 10, obtained from the centrifuging step in the Amott test. In this method, Gatenby and Marsden (1957) suggested to determine wettability by the correlation between the wetting degree and the areas under the capillary pressure curves. Although the USBM is a faster method and more sensitive near neutral wettability it cannot determine fractional nor mixed-wetting systems which in some cases the Amott test can (Ghedan et al., 2010).

While in an Amott test both forced and spontaneous imbibition are used, only forced imbibition is performed in the USBM method. The core is first prepared for the test by centrifuging under oil until reaching S_{wi}, similarly to the Amott test. After this preparational step the core undergoes another centrifugation but this time under brine. The centrifugation is carried out by increasing the speed incrementally until reaching -10 psi capillary pressure. This step is known as brine drive. The average saturation of the core during brine drive is measured at each incremental capillary pressure and plotted forming curve I in Figure 10. The next step is called oil drive where the oil displaces the brine by forced imbibition. Same measurements are performed as during brine drive, the average saturation vs capillary pressure at each increment is plotted until reaching 10 psi forming curve II. The ratio of the areas, A1 and A2, under the capillary pressure curves is used to calculate the wettability index as follows:

$$WI_{USBM} = \log\left(\frac{A_1}{A_2}\right) \tag{2.15}$$

Where,

WI_{USBM} Wettability index from USBM method

A_1 Area under oil drive curve

A_2 Area under brine drive curve

For a preferentially water-wet core A_1 is larger than A_2 giving W > 0, for neutral-wet core A_1 and A_2 are near or equal meaning W will be near or at 0 and for oil-wet core A_1 is smaller than A_2 giving W < 0. The greater the wetting preference the larger the absolute value of W becomes (Anderson, 1986). Even though theoretically W can range from $-\infty$ to $+\infty$ the observed values have been in range from -2 to $+2$ (Strand et al., 2006b).

2.5.5. Chromatographic Wettability Test

Chromatographic wettability test is a new method developed by Strand et al. (2006) that measures the wettability conditions of chalk cores. Performing an Amott test is not that effective as it is unsensitive near neutral wetting conditions neither is the USBM test due to its lack of determination of mixed or fractional wetting conditions. Both Amott and USBM test methods are based on forced and spontaneous imbibition processes where saturation is the measured parameter. A chromatographic wettability test focuses on the surface chemistry aspect of wettability, and it is based on chromatographic separation of two water-soluble components: a potential determining ion towards chalk surface, SO_4^{2-}, and a tracer that is a non-adsorbing water tracer such as thiocyanate, SCN^-.

The first step in a chromatographic wettability test is to establish S_{or} in the oil aged core by flooding the core with a brine that does not contain SCN^- and SO_4^{2-}. After reaching S_{or}, the core is flooded with a minimum of 2 PV with brine containing SCN^- and SO_4^{2-}. During this step, fractions of 1-3 ml of the effluent is collected by a fraction collector and the volume and PV are calculated by using the fluids density and weight for each fraction. The concentrations of SCN^- and SO_4^{2-} in the effluent fractions were then analysed using ion chromatograph analysis. The relative concentrations of both components were then plotted against injected pore volumes. The delay that occurs between the two curves is proportional to the rock surface that is available for adsorption. The wettability index obtained from chromatographic wettability test, WI_{CWT}, is found by the area ratio of SCN^- and SO_4^{2-} curves, A_{wett}, over the area of a core containing heptane, $A_{heptane}$, which is the reference representing a completely water-wet system. WI_{CWT} is given by the following equation:

$$WI_{CWT} = \frac{A_{wett}}{A_{heptane}} \tag{2.16}$$

Where,

A_{wett} Area ratio of thiocyanate and sulphate

$A_{heptane}$ Reference area from a completely water-wet core saturated with heptane

The value of WI_{CWT} will range from 0 to 1, where 0 corresponds to a completely oil-wet system, 0.5 corresponds to neutral-wet system and 1 is a completely water-wet system. What is unique about this test is that it can be conducted fast compared to Amott test where performing a spontaneous imbibition is necessary and it is sensitive to neutral wettability.

3. Wettability Alteration by Smart Water in Carbonate Reservoirs

3.1. Carbonate Reservoirs

Almost 60% of oil and 40% of gas reserves is estimated to be held in carbonate reservoirs worldwide where it is dominated in the Middle East holding up to 70% oil and 90% gas reserves (Schlumberger). Carbonates reservoirs are highly heterogenous with a porosity ranging from 1 up to 45% and permeability in the range of 0.01 millidarcy (md) to 1.0 darcy. To produce oil from a reservoir, a minimum permeability of 0.1 md is needed (Lucia, 2007). One of the largest carbonate reservoirs in the Norwegian continental shelf is found in Ekofisk field. Ekofisk lies in a naturally fractured chalk reservoir with low matrix permeability (1-10 md) and high porosity (30-45%) (Austad et al., 2008). The average oil recovery for carbonates is usually less than 30% (Puntervold et al., 2009). The combination of high oil reserves and a low recovery factor makes carbonate reservoirs an interesting field of research to improve the oil recovery especially by low cost EOR-methods.

3.1.1. Carbonate Rocks

The term carbonates refer to the anionic complex of $(CO_3)^{2-}$ and the divalent metallic cations where Ca^{2+}, Mg^{2+} and Fe^{2+} are the most common. The atoms in carbonates can be arranged in three different ways forming crystal lattice structures that either gives a hexagonal, orthorhombic, and monoclinic crystal systems. Calcite $(CaCO_3)$ is a well-known carbonate that crystallize in the hexagonal system. Aragonite $(CaCO_3)$ is another carbonate rock with the same chemical formula but is crystallized in the orthorhombic system. Aragonite is mostly found in modern oceans and rarely found in reservoirs leaving us with calcite and dolomite $CaMg(CO_3)_2$ minerals as the most common carbonate in reservoirs that makes up to 90% of naturally occurring carbonate worldwide (Ahr, 2008). A reservoir is characterized as carbonate reservoir when it contains more than 50% carbonate minerals. There are two common types of carbonate rocks: limestone and dolomite. A rock is characterized as limestone when it contains

more than 50% calcite, and as dolomite when it contains more than 50% dolomite (Bissell and Chilingar, 1967).

Carbonate rocks are formed by accumulation of bioclastic sediments on the seabed along with small amounts of chemical precipitation. The bioclastic sediments are broken shells from calcareous organisms such as coral, clams and algae and occur only in a marine environment with clear, warm, and shallow water. This environment is the only environment where calcareous algae and corals can thrive (Wilson, 1975). Carbonate rocks are also called biogenic as most of the carbonate rocks originates from biological activity. Most of the carbonates exists below the latitude of 30° south and north the equator, see Figure 11.

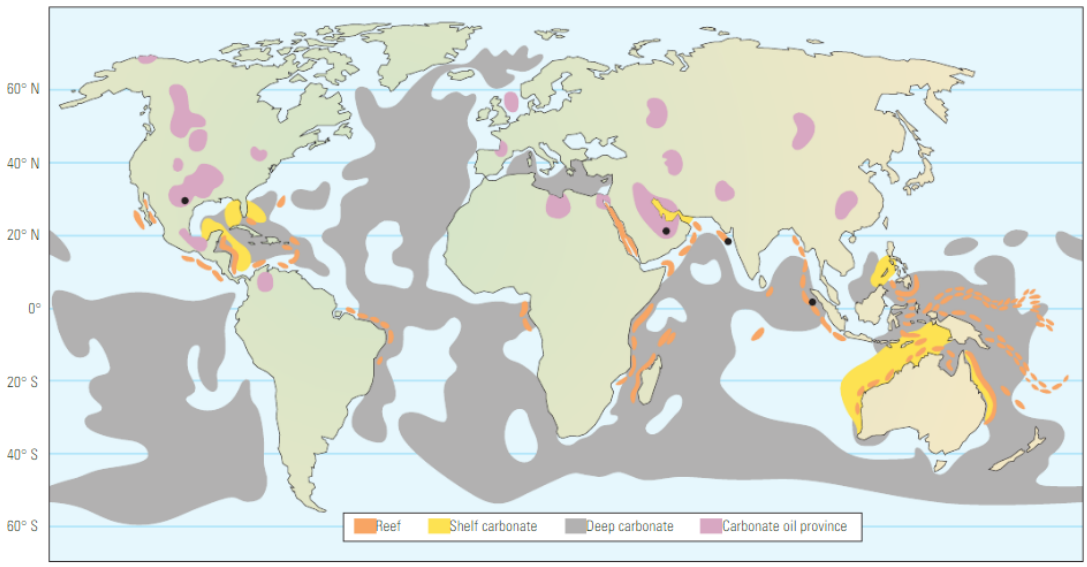

Figure 11: Distribution of carbonate rocks where reef shelf carbonate, deep carbonate and carbonate oil reservoirs are presented by the colour orange, yellow, grey, and purple, respectively.

After deposition the sediments undergoes a diagenesis process where chemical and physical changes take place forming a solid carbonate rock. This process has a huge impact on pore space and permeability of the rock in addition to its texture which leads to a huge variety in rock properties (Akbar et al., 2000). A paper published by Chilingar and Yen (1983) examined the wettability of 161 carbonate reservoir cores where they found that 15% of the cores were strongly oil-wet, 65% were oil-wet, 12% were neutral-wet and only 8% were water-wet, Figure 12. With this result we can indicate that the majority of carbonate reservoir are preferentially oil-wet.

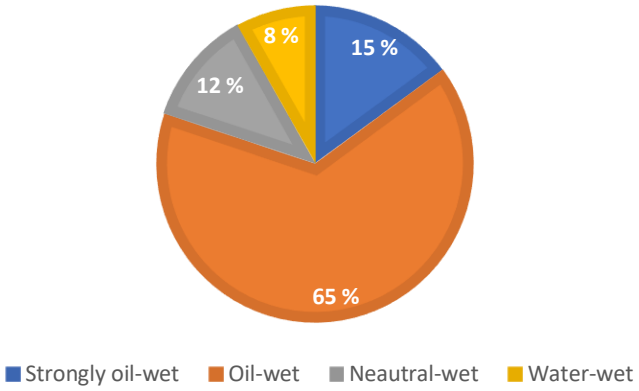

Figure 12: Wettability distribution of 161examined carbonate reservoir cores showing that 80% of the cores are either oil-wet or strongly oil-wet

Chalk

Chalk rocks is a pelagic sediment that consist of coccolith skeletal fragments coming from coccolithophorids, a yellow-green algae, See Figure 13. When coccolithophorids dies they break down into disk-shaped particles with a diameter of 2-20 µm before sinking down to the seabed (Ahr, 2008). Chalk reservoirs are usually pure ($CaCO_3$), but some clay-rich intervals may also occur like the Plenus Marl formation in North Sea where it forms a tight low-permeable formation. Chalk rocks contain micropores that makes the porosity as high as 40-50%, but with very low permeability, around 1 md, due to low pore-throat diameter. In Ekofisk, the chalk reservoir is combined with another pore type, fractures, that increase the reservoirs permeability making oil production much more productive (Bjørlykke, 2015).

.

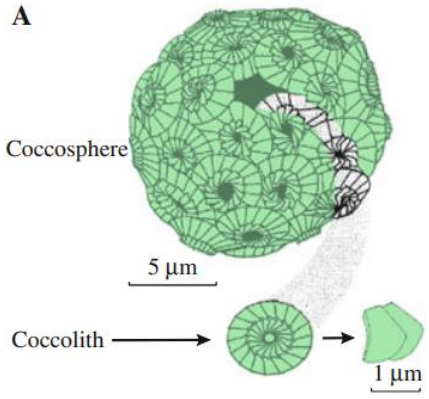

Figure 13: A coccosphere coming from the yellow-green algae coccolithophorids. The skeletal fragments are called coccolith.

3.2. Initial Wettability of Reservoir Chalk

The initial wettability in a reservoir is of great importance when it comes to reservoir management and indication of the potential effect of an EOR method. The initial wettability of carbonate reservoir along with its heterogeneity have a huge impact on the oil recovery. The are several factors that affect the initial wettability of reservoir chalk such as, water-film stability, temperature, initial presence of sulfate, presence of cations in formation water and the amount of acid polar components in crude oil.

Most reservoirs are initially considered as water-wet before migration of oil. When oil migrates into a preferentially water-wet reservoir it will saturate the reservoir gradually where we get most saturation at the top with irreducible water then the saturation decreases gradually until free-water level, see Figure 14. If the oil migrates into a preferentially oil-wet reservoir the saturation profile will be different with a maximum saturation until reaching the free-water level. The oil saturation will then start to decrease drastically compared to the saturation profile found in a water-wet reservoir. The distribution of the saturation profiles is determined by the capillary pressure between these two immiscible fluids (Abdallah et al., 2007).

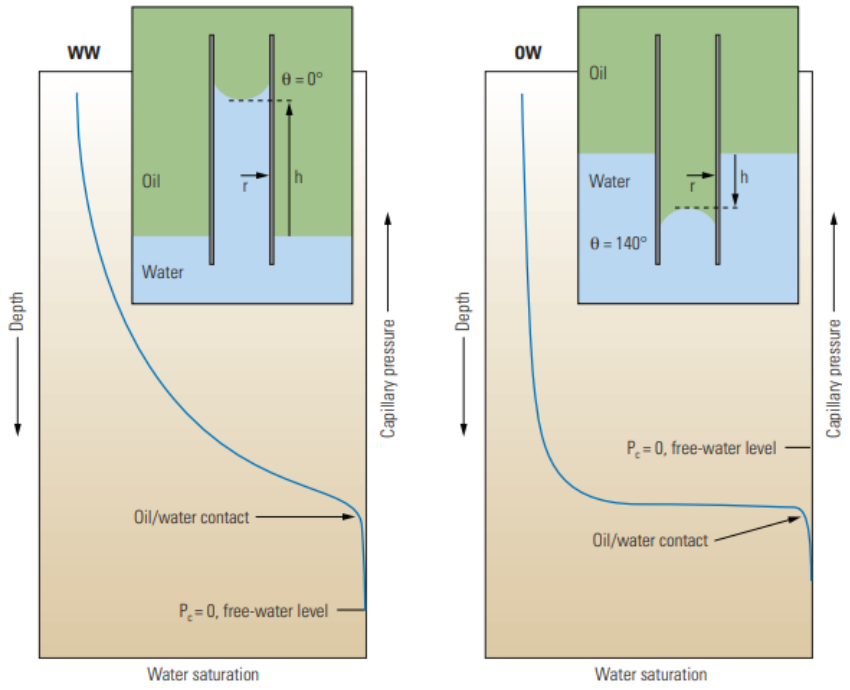

(a) (b)

Figure 14: Distribution of saturation in (a) water-wet reservoir and (b) oil-wet reservoir determined by the capillary pressure between water and oil.

Water-film Stability and the Effect of AN

The wettability in an oil/brine/rock system has often been linked to the thickness of the water-film that covers the rock surface which is determined by how stable the forces within the film are. These forces generate a pressure called the disjoining pressure that maintains and prevents the film from becoming any thinner when it is equal to the capillary pressure. A large disjoining pressure is favourable as it maintains a water-wet system. Low disjoining pressure leads to drainage of the water-film making the system oil-wet (Dubey and Doe, 1993). When oil migrates into a reservoir it will partially displace the water resulting in an oil/water/rock system with oil-water and water-solid interfaces. These two interfaces can have positive or negative charge. For oil-water interface the charge is negative due the presence of carboxylic acid in the crude oil. For water-carbonate interface the charge is positive due to high concentration of Ca^{2+} cation in the water-film as well as a pH value < 9.5. Since the interfaces have opposite charges, they will attract each other making the water-film unstable enough for the oil to be in contact with the carbonate surface. Once the oil contacts the surface, resins and asphaltenes which represent the carboxylic group will adsorb strongly onto the carbonate surface and thus decreasing the water-wetness of the system. Therefore, the

acid number in crude oil has a great influence on carbonates wetting state where the water wetness decreases as the AN increase (Zhang and Austad, 2005).

Research conducted by Standnes and Austad (2000) showed how the number of carboxylic acid groups in the oil impacts the wettability of the chalk. The negatively charged carboxylic acid groups in the oil adsorbs onto chalks surface making it less water wet. Chalk cores were saturated with crude oils with different AN number and spontaneous imbibition test were performed to evaluate the wettability. Figure 15 shows that oil A with AN =0.0 gives the highest oil recovery. The oil recovery decreases with increasing AN.

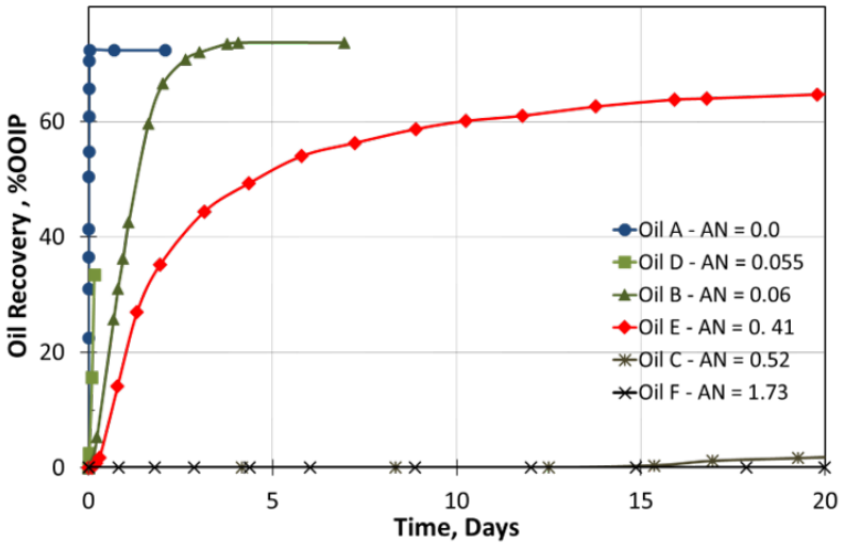

Figure 15: Spontaneous imbibition test performed on chalk cores saturated with crude oil with different AN. Oil recovery decreases with increasing AN (Standnes and Austad, 2000).

The Effect of Cations

In addition to AN, a recent study by Shariatpanahi et al., (2016) showed how the cations influences the initial wetting state of chalk. Spontaneous imbibition test was used to indicate the initial wetting properties of Stevns Klint chalk cores. The experiment was carried out at 25°C with different brines and saturated with the same oil with AN = 0.17 mgKOH/g. In this experiment, the saturated brine was also used as the imbibing brine. The following brines was tested: $MgCl_2$, $CaCl_2$, NaCl, VB0S and DI-water. All brines had the same salinity so that the only focus of this experiment will be the effect of cations. The results obtained by this study is shown in Figure 16 below where it is presented as the oil recovery, % of OOIP vs time.

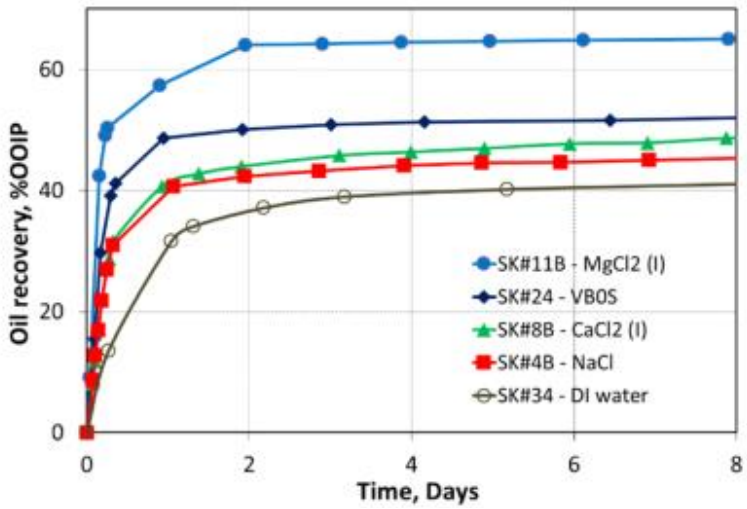

Figure 16: Effect of FW with different composition on the initial wettability of chalk. Spontaneous imbibition test performed at 25°C on Stevns Klint chalk cores. The cores were saturated with 10% FW and 90% oil with AN=0.17 mgKOH/g. Figure by (Shariatpanahi et al., 2016)

Based on the obtained results, the core with saturated and imbibed $MgCl_2$-brine has the highest initial water wetness and produced most oil with 65% of OOIP. The lowest initial water wetness belonged to the core that is saturated and imbibed with DI-water. Only 40% of OOIP is recovered out of this core. The reason for low initial water wetness for DI-water might be due to the lack of ionic double layer that gives more access for the negatively charged carboxylic acid to break the water-film and contact the chalk rock surface. The study also concludes that formation water with high Mg^{2+} concentration leads to adsorption onto the chalk rock preventing the carboxylic acid to contact the chalk surface and thus resulting in high initial water wetness. Since carboxylic acid have more affinity towards Ca^{2+} the brine with Ca^{2+} will initially be less water-wet than Mg^{2+}.

Initial Sulphate and Wettability

Another parameter that plays a major role on the initial wetting state of chalk outcrop rock is the initially present SO_4^{-2}. A study performed by Puntervold et al., (2017) showed how initially present sulphate impacts the initial wettability. Two Stevns Klint chalk outcrop cores went through spontaneous imbibition test. Prior to establishment of initial water saturation, one of the cores were cleaned by flooding DI-water to remove SO_4^{-2} on the chalk surface while the other remained uncleaned. Both cores went through the same restoration process before performing spontaneous imbibition test. The results

showed that the uncleaned core recovered 70 % of OOIP while the cleaned core gave a 30 % recovery of OOIP. The cores went further through a chromatographic wettability test that resulted in a wetting index WI_{cwt} = 0.84 for the uncleaned core indicating very water-wet chalk core. The cleaned core had a WI_{cwt} = 0.65 which indicated neutral to slightly water-wet wetting conditions. These results concludes that the cleaned core is less water-wet and mimics the wetting conditions found in a reservoir more than the uncleaned one. Having SO_4^{-2}-ions initially present on chalk surface may already have altered the wettability towards more water-wet conditions so that when evaluating for Smart Water the wettability alteration may be at a minimum or even absent and the results are not representative. This conclusion applies only to outcrop cores and are of great importance when evaluating Smart Water EOR for real field reservoirs.

3.3. Potential Determining Ions in Chalk

By measuring the electro-kinetic mobility of calcite particles in aqueous solution as a function of pH it was found out that both Ca^{2+} and SO_4^{2-} acted as a potential determining ions towards the calcite surface (Pierre et al., 1990) . In 2006, Strand et al. measured the zeta potential of the chalk to evaluate the electric charge of carbonates, see Figure 17. The zeta potential measurement was executed on 4 wt% of milled chalk in NaCl brine with varying concentration ratios of Ca^{2+} and SO_4^{2-}.

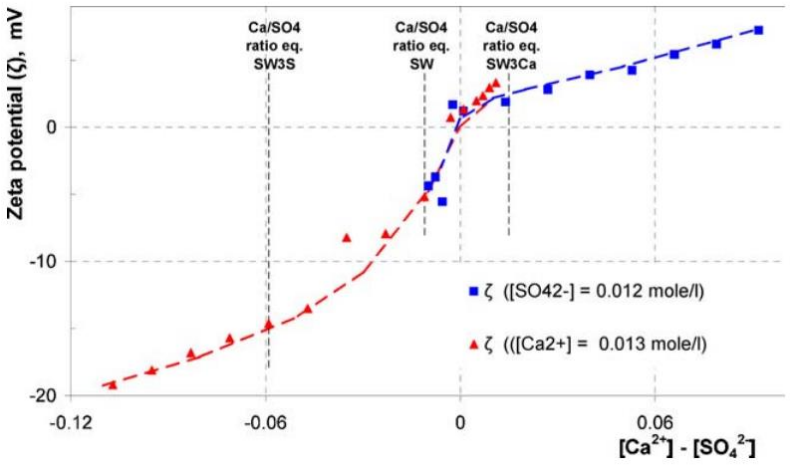

Figure 17: Zeta potential measurements as a function of concentration difference $[Ca^{2+}]$ — $[SO_4^{2-}]$. The blue plot represents the NaCl brine with constant SO_4^{2-} and varying Ca^{2+} whereas the red plot represents the NaCl brine with constant Ca^{2+} concentration and varying SO_4^{2-} (Strand et al., 2006a).

It appeared that the zeta potential was close to 0 when the concentration difference $[Ca^{2+}]$ — $[SO_4^{2-}]$ is equal to 0, positive zeta potential when $[Ca^{2+}]$— $[SO_4^{2-}] > 0$ and negative zeta potential when $[Ca^{2+}]$ — $[SO_4^{2-}] < 0$. A positive zeta potential indicates a positive charge on the chalk surface whereas a negative zeta potential indicates a negative surface charge. Hence the surface charge of chalk seems to be controlled by the relative concentration of the two potential determining ions.

The two potential determining ions including Mg^{2+} was then studied further by Strand et al. (2006) to gain broader understanding of how they interact with each other. Viscous flooding was performed on a Stevns Klint chalk core, and the ion concentration of the effluent was analysed, Figure 18. The concentration profile of SO_4^{2-} is delayed by 0.1 PV compared to the concentration profile of the tracer, SCN^-, indicating adsorption onto the chalk surface.

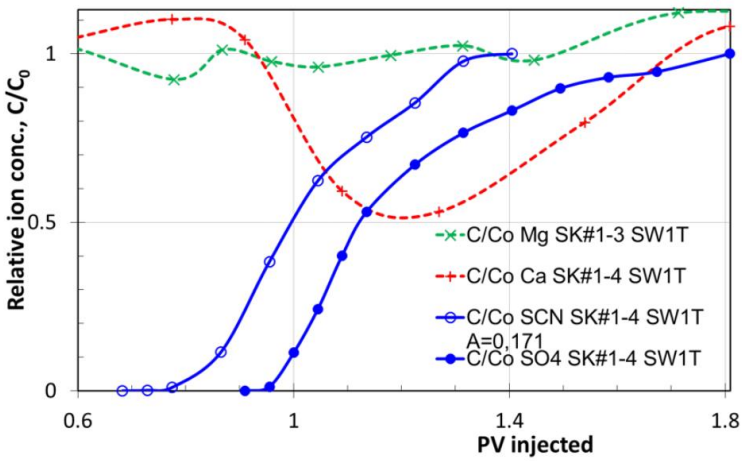

Figure 18: Relative concentration of Mg^{2+}, Ca^{2+}, $SO_4^{2-}$and SCN^- in effluent vs. PV injected. Viscous flooding experiment conducted on Stevns Klint chalk core.

Once the concentration profile of SO_4^{2-} appears, the concentration of Ca^{2+} decreases. This is believed to be due to co-adsorption of Ca^{2+}-ions onto the already adsorbed SO_4^{2-}. No significantly changes are observed in the concentration profile of Mg^{2+}. This may indicate that Mg^{2+} is a very weak potential determining ion than Ca^{2+}. Based on what is observed, it seems like there is a symbiotic interaction between SO_4^{2-} and Ca^{2+} that alters the wettability in chalk and that Mg^{2+} does not involve directly in the wettability alteration process.

Wettability alteration induced by Mg^{2+} was however proved by Zhang et al. (2006) to take place at high temperatures, T_{res} > 70°C. An experiment was performed to analyse the concentration of the potential determining ions in the effluent at various temperatures. A chalk core initially saturated with SW was flooded with SW at a rate of 1 PV/day. After analysing the concentrations, it was found out that Mg^{2+} could substitute Ca^{2+} on the chalks surface when the temperature exceeds 70°C due to higher Ca^{2+} concentration in the effluent, see Figure 19.

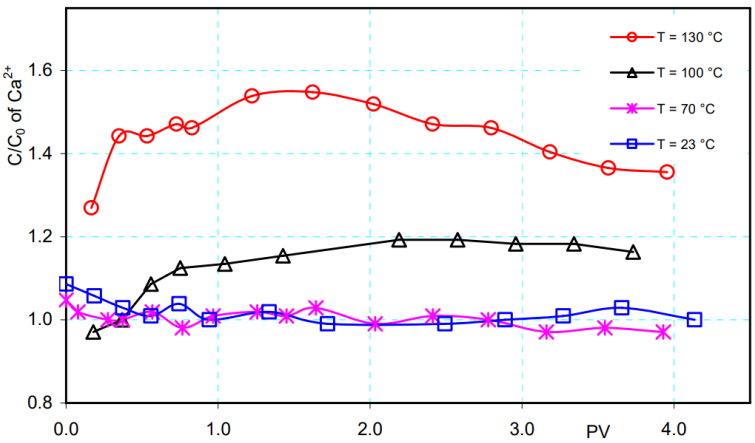

Figure 19: Ca^{2+}concentration in the effluent vs PV injected. The core was initially saturated and flooded with SW at a rate of 1PV/day (Zhang, 2006).

The results obtained from all this research concludes that there are three potential determining ions that are the key parameters in wettability alteration process in chalk rock. The catalyst in this process is SO_4^{2-} by adsorbing onto and lowering the positively charged chalk surface allowing the Ca^{2+} to co-adsorb onto SO_4^{2-} and displace the carboxylic acid from the surface (Zhang, 2006). The suggested mechanism behind this wettability alteration in chalk by Smart Water is presented below.

3.4. Smart Water Mechanism

Smart Water is a brine with specific ion composition that alters the wettability of carbonate rock towards more water-wet conditions in order to improve the oil recovery. The mechanism behind Smart Water only takes place in aqueous conditions where SO_4^{2-} -ions are active and the carbonate rock is in contact with water allowing the SO_4^{2-} to be adsorbed (Pierre et al., 1990). The adsorption of SO_4^{2-} will lower the positive surface charge of the chalk surface resulting in reduction of the electrostatic repulsive force allowing more Ca^{2+} to attract towards the surface. A reaction between Ca^{2+} and the strongly adsorbed carboxylic acid ($RCOO^-$) in the oil will occur resulting in carboxylic acid to be detached and displaced away from the chalks surface. The following reaction expresses the described mechanism:

$$RCOO—CaCO3s + Ca2 + + SO42 - = RCOOCa + + CaCO3s + SO42 - \quad (3.1)$$

The $SO42—$ion in this reaction acts as a catalyst by increasing the amount of Ca^{2+} close to the surface (Austad et al., 2009). A numerous of experiments have been conducted to study the effect of brines consisting of only $SO42—$ions. These experiments confirmed that SO_4^{2-} alone is not able to trigger wettability alteration and that the effect is caused by a symbiotic interaction between SO_4^{2-}, Ca^{2+} and the positively charged chalk surface(Austad et al., 2009; Strand et al., 2006a).

In 2006, Zhang et al. found that Mg^{2+} also contributed to the alteration of wettability at high temperatures, T > 70°C, where Mg^{2+} were able to substitute Ca^{2+} at the chalk surface. In 2009 Austad et al (2009) suggested that Mg^{2+} substitutes and displace both Ca^{2+} that are connected to the carboxylic acid and other nonconnected Ca^{2+} from the chalk surface. Thus, a small increase in oil recovery will take place. This reaction is till governed by the SO_4^{2-} -ion. The displacement of Ca^{2+} by Mg^{2+} is expressed in the following reaction:

$$RCOO—CaCO3s + Mg2 + + SO42 - = RCOOCa + + MgCO3s + SO42 - \quad (3.2)$$

An illustration of how the Smart Water mechanism works is presented in Figure 20 below:

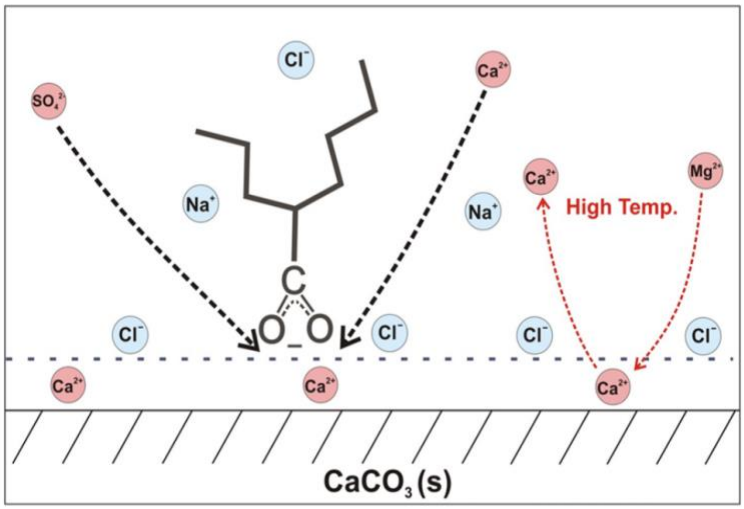

Figure 20: A schematic illustration of Smart Water mechanism. The active ions at low temperature are $SO_4^{2-}$and Ca^{2+}whereas at high temperature Mg^{2+} becomes active

3.5. Temperature Effect on Wettability Alteration

Since temperature affects the reactivity of the potential determining ions, it is considered to be the most important parameter in wettability alteration. When the ionic compounds dissolve in water they will attract water molecules, H_2O. As a result of this attraction each ion will be surrounded by H_2O to form hydrated ions. If the ion is positively charged like Ca^{2+} or Mg^{2+}, the negative side (oxygen) of the water molecule will face the ion. Similarly, when a negative charged ion, such as SO_4^{2-}, is introduced to water, the positive side (hydrogen) of the water molecule will be facing the ion. The ion can be surrounded by several water molecules creating a rigid structure due to the ion-dipole force. This water molecule structure lowers the reactivity of the ion remarkably. The water creates a strong ion-dipole attraction making the hydration reactions exothermic and thus temperature dependent (Burton, 2000). During hydration of Mg^{2+}, heat will be released as expressed by the given reaction:

$$Mg^{2+} + 36H_2O \leftrightarrow [Mg(H_2O)_{36}]^{2+} + Heat \tag{3.4}$$

When a Mg^{2+}-containing brine is exposed to heat, the reaction will, according to Le Châtelier's principle, move towards left making Mg^{2+} less hydrated. Thus, the reactivity of Mg^{2+} in the brine will increase. Strand et. Al., (2006) showed how hydrated SO_4^{2-} are affected by temperature by studying the chromatographic separation of the nonadsorbing SCN^- and SO_4^{2-}. The results, Figure 21, showed that the area between the corresponding SCN^- and SO_4^{2-} curves increased with temperature because of delay in the effluent concentration profile of SO_4^{2-} due to adsorption onto the chalk surface. The higher the temperature the less hydrated and more reactive SO_4^{2-} become. The water structure surrounding the ions usually breaks around the 100°C and therefore it is hard to induce wettability alteration at temperatures lower than 90°C due to hydration (Strand et al., 2008).

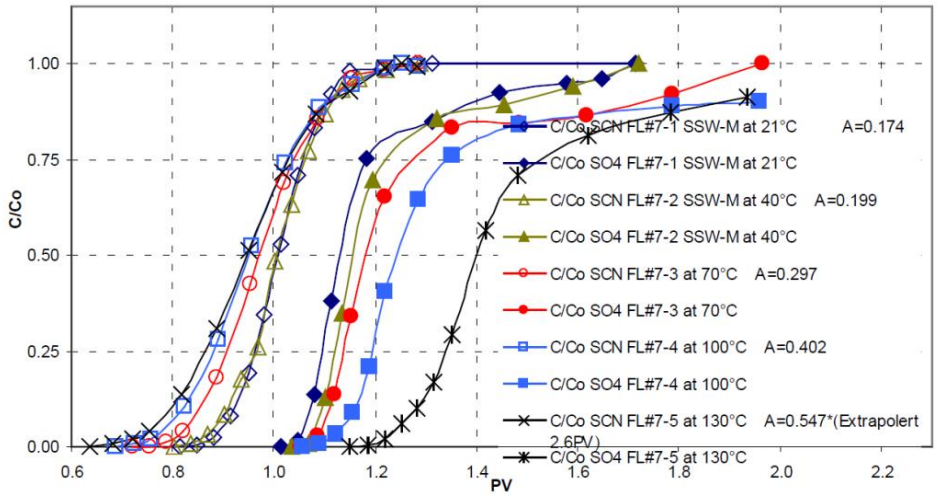

Figure 21: Chromatographic separation of the nonadsorbing SCN^- and SO_4^{2-} showing an increase the area between SCN^- and SO_4^{2-} as the temperature increases (Strand et. Al., 2006).

Spontaneous imbibition with SW at various SO_4^{2-} concentration was performed by (Zhang, 2006) at different temperatures. SI performed at 70°C and 90°C are presented in Figure 22 below. All corresponding brines had a significantly improvement of OOIP at 90°C compared to at 70°C.

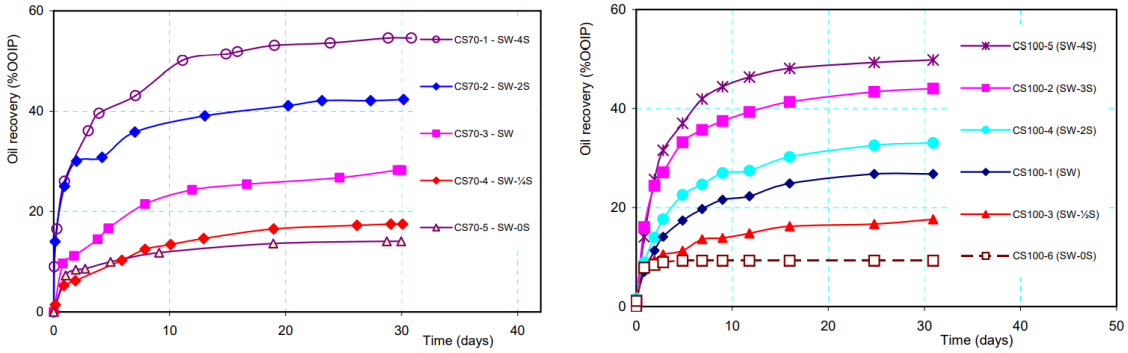

(a) (b)

Figure 22: Spontaneous imbibition on chalk cores with SW at various SO_4^{2-} where (a) are the SI profiles at 70°C and (b) are the SI profiles at 90°C.

3.6. Modified Seawater for EOR

A well know Smart Water EOR fluid that induces wettability alteration in carbonates is seawater. SW increases the water-wetness of chalk which causes an increase in oil recovery. In 2012, Fathi found out that modifications of SW can result in oil recovery that is beyond the recovery obtained by the standard SW due to wettability alteration to more water wet conditions. Some of the suggested modifications were spiking SW with different concentrations of SO_4^{2-}. Another suggested modification was removing NaCl from SW.

Both brines were then used in a spontaneous imbibition test to evaluate their performance in wettability alteration, see Figure 23.

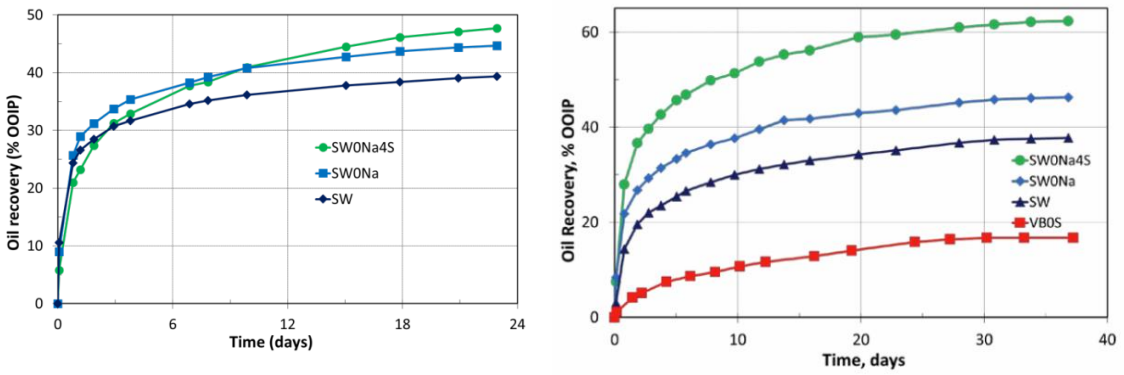

(a) (b)

Figure 23: Oil recovery by spontaneous imbibition with modified SW at (a) 70°C and (b) 90°C. The standard SW is compared with SW depleted in NaCl and SW spiked with 4 times SO_4^{2-} at two different temperatures. Figures from (Fathi, 2012)

By varying the amount of NaCl and SO_4^{2-} in SW, the effect of the monovalent $Na^+$and SO_4^{2-} concentration could be studied. Three brines were compared with each other: standard SW, SW completely depleted of NaCl termed as "SW0Na" and SW spiked with 4 times SO_4^{2-} and depleted in NaCl termed as "SW0Na4S". Oil recovery increased as the temperature increased from 70°C to 90°C. The highest oil recovery in both 90°C and 70°C were obtained by using SW0Na4S as the imbibition brine. According to Fathi (2012) The increase in recovery is due to better accessibility for the potential determining ions to interact with the chalk surface. Both Na^+ and Cl^- are present in the double layer where the presence of Na^+ will reduce the accessibility of Ca^{2+} and Mg^{2+} and the presence of Cl^- will reduce the accessibility of SO_4^{2-} at the surface. When removing NaCl from SW the access for the potential determining ions to the chalk surface will increase resulting in an increase in both imbibition rate and oil recovery.

At 70°C the SW0Na4S increases the oil recovery by approximately 8-9% of OOIP compared to the standard SW. The increase is significantly higher at 90°C with over 20% of OOIP. It appears that at higher temperature SO_4^{2-} get more active due to less hydration as discussed in chapter (3.5). Combining this with the absence of NaCl, the oil recovery obtained is significantly higher.

In 2015, Puntervold et al. studied the degree of modification SW needs to obtain a significant increase in oil recovery by how much removal and addition of NaCl and SO_4^{2-}, respectively, is needed. Spontaneous imbibition test was conducted at 90°C using two different cores for each imbibition brine. SW with varying amount of NaCl from 0-100% relative to SW and completely NaCl-depleted SW with increased SO_4^{2-} concentrations of 0-4 times the concentration in SW were used as the imbibition brines. The results from SI test are shown in Figure 24.

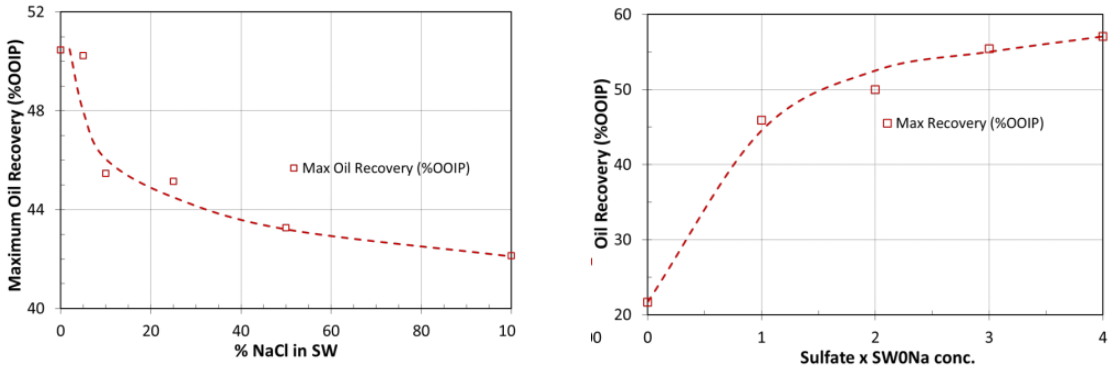

(a) (b)

Figure 24: Oil recovery vs SW composition. The spontaneous imbibition test was conducted at 90°C using cores with $S_{wi} = 10\%$ and $S_{oi} = 90\%$ oil with AN=0.5 mgKOH/g. Figure (a) shows the maximum oil recovery as a function of %NaCl in SW. Figure (b) maximum oil recovery as a function of times SO_4^{2-} concentration in SW (Puntervold et al., 2015).

The results showed that to observe a significant effect in oil recovery, a significant amount of NaCl must be removed. The oil recovery decreases linearly between 50 and 100% NaCl in SW with only 2-3% difference in oil recovery. When removing 90% NaCl in SW the SI profile increases significantly. The results obtained in Figure 24b shows that spiking SW with 1-4 times SO_4^{2-} the increase in oil recovery is low. The difference between 1xSO_4^{2-} and 4xSO_4^{2-} is only 10% increase in oil recovery.

3.7. Production of Smart Water

3.7.1. Smart Water production by membranes

A filtration process is when a fluid stream passes through a filter where one or more particles are separated due to size difference (Cheryan, 1998). When immiscible solid particles are separated from a fluid, it is referred to as filtration. In order to filter out particles in the ionic range (1-10 Å), membrane filters are required. Membrane filters acts as a selective barrier meaning they permit passage of specific components and retain other specific components in a solution. A recent study by Nair (2019) proposed the possibility of producing Smart Water by using nano-filtration (NF) membranes. The idea was to desalinate SW and produced water in the field to obtain Smart Water composition. Pressure-driven filters are used to force SW through a semi-permeable membrane. When SW passes through it splits into retentate- and permeate stream as illustrated in Figure 25 below.

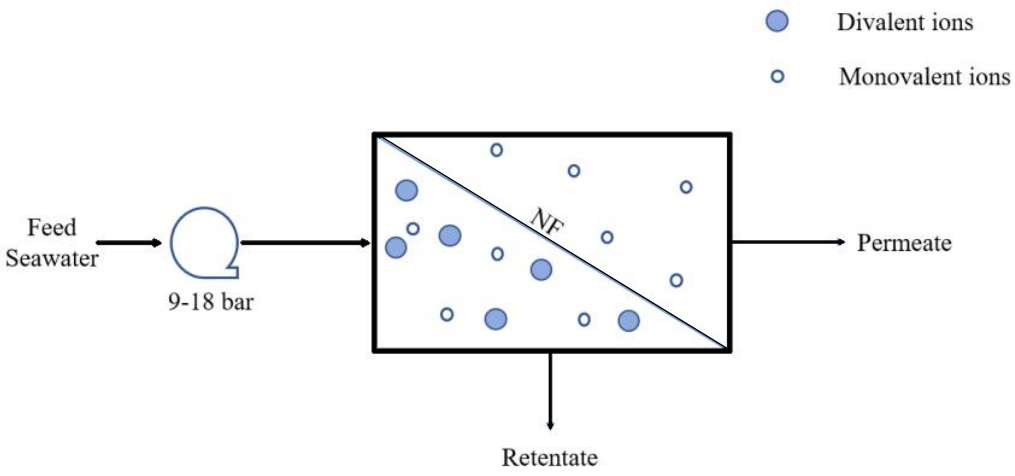

Figure 25: Smart Water production by using nano-filtration membrane.

After passage of SW through the membrane, the retentate is now depleted from monovalent ions but enriched with divalent ions making it suitable to be used as Smart Water in carbonate reservoirs while the permeate has a low concentration of the divalent ions and can be used in sandstone reservoirs. However, the NF membranes used in the study were not effective. A high amount of Ca^{2+}, around 30-45%, was permeated through the membrane. Ion rejection at different pressures is displayed in Figure 26.

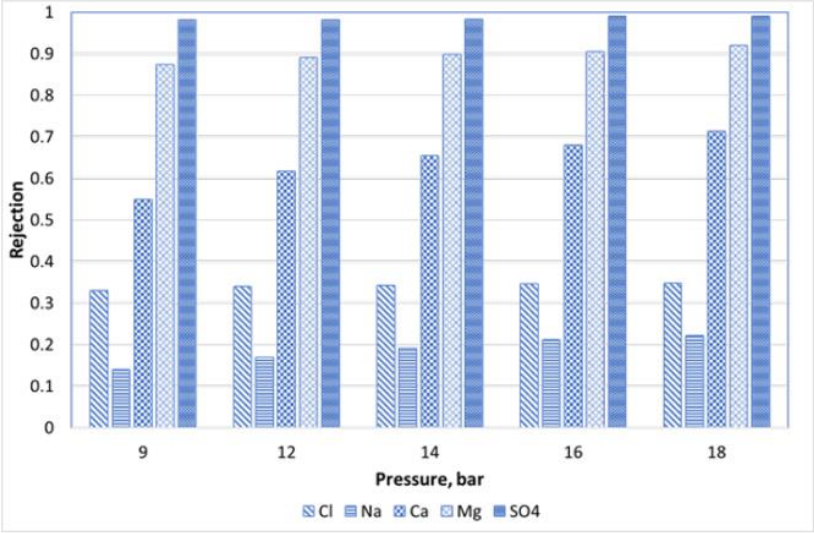

Figure 26: Ion rejection by NF membrane at different pressures.

The effect of Smart Water is basically based on Ca^{2+} being co-adsorbed onto SO_4^{2-} as discussed in chapter (3.3). It is therefore important to not lower the concentration of Ca^{2+} as it causes an imbalance between the two important potential determining ions.

4. Experimental

In this experimental section, materials, instruments, and methodology to conduct the experiment are presented.

4.1. Materials

A brief description of the procedure used to obtain the final materials along with certain properties are given under this section. The materials are later used to perform the main experiments in this thesis.

4.1.1. Core Materials

The chalk outcrop Stevns Klint located near Copenhagen in Denmark were used to resemble the North Sea reservoir chalk. This outcrop is an excellent analogue to the reservoir chalk in the Norwegian continental shelf as it has the same material properties like porosity, permeability and wetting conditions (Frykman, 2001). The chalk cores were drilled out from the same chalk outcrop block, Figure 27. They were then dried, shaven, cut and trimmed down to the desired diameter and length. The measured and calculated properties are summarized in the table below:

Table 1: Physical properties of Stevns Klint cores

Core	L (cm)	D (cm)	V_b (cm^3)	PV (ml)	φ (%)	k (mD)
SK1	7.00	3.80	79.39	38.58	48.59	4.08
SK2	7.10	3.80	80.52	39.09	48.55	4.70
SK3	7.06	3.80	80.07	39.05	48.78	3.80
SK4	7.24	3.81	81.66	40.07	49.16	3.84
SK5	7.03	3.76	77.56	41.35	49.30	4.08
SK6	6.93	3.80	80.09	38.64	49.16	4.70
SK7	7.05	3.80	79.96	37.92	47.42	3.81
SK8	7.02	3.80	79.61	39.95	50.18	3.84

(a) (b) © (d)

Figure 27: Chalk cores drilled out from the same chalk outcrop block (a). They were then shaven (b), cut in half (c), and trimmed (d) to the desired length.

4.1.2. Preparation of Oil

The crude oil that is used in this study is from Heidrun field with a very high acid number (AN). To observe any wettability alteration in chalk cores it is desired to establish slightly water-wet conditions. To obtain this condition the AN must be reduced. Description of the process of preparing the crude oil to a lower AN is given under this section.

Preparation of RES-40

The RES-40, our base oil, was prepared by diluting crude oil with n-Heptane, to lower the crude oils viscosity, in the ratio of 60/40 by weight respectively. 10 wt% of Silica Gel was then added to the crude oil mixture and stirred at room temperature for 3 days. An equal amount of Silica Gel was then added, and the mixture was stirred for two additional days. Silica Gel is used due to its ability to extract the polar oil components out of the crude oil hence lowering AN and BN. The mixture was then centrifuged twice, as it optimizes the filtering step, with Megafuge ST Plus Series Centrifuge to separate the adsorbed Silica Gel with the polar oil components from our RES-40 oil. The centrifuge was set at a speed of 3000 rpm with a duration of 15 minutes at a temperature of 22 °C. The acceleration and the deceleration were both set at a value of 9. Bucket number used was 3608. After centrifuging the RES-40 oil was filtered with 8µm Millipore filter and stored in dark flasks. The measured values of RES-40 are presented in table 2 below.

Preparation of Oil A

Once the RES-40 is prepared, it is now ready to be mixed with RES-40-0, an oil with AN=0. This step lowers the AN of RES-40, the more RES-40-0 added the lower the AN of oil A would be. The target AN, which in our case is 0.6, is calculated as follows:

$$\text{Target AN} = \text{AN}_{\text{RES}-40} \cdot \frac{\text{V}_{\text{RES}-40}}{\text{V}_{\text{RES}-40+\text{RES}-40-0}} + \text{AN}_{\text{RES}-40-0} \cdot \frac{\text{V}_{\text{RES}-40-0}}{\text{V}_{\text{RES}-40+\text{RES}-40-0}} \qquad (4.1)$$

The AN and the base number, BN, of the final oil was measured using Mettler Toledo T50 Titrator. Properties of the oil is given in table 2. This oil was used in this study to saturate the chalk cores.

Table 2: Oil properties of RES-40, RES-40-0, and Oil A. See chapter (4.2) for mythology

Oil	ρ (g/ cm^3)	AN (mgKOH/g)	BN (mgKOH/g)	$\mu_{23°C}$ (mPa·s)
RES-40	-	2.18	0.66	-
RES-40-0	-	0	0.05	-
Oil A	0.8069	0.58	0.30	2.460

4.1.3. Polysulphate (PS)

The PS used in this study comes from polyhalite rock layer located 1000 m below the North Sea near the North Yorkshire coast in the UK. The deposition of this polyhalite occurred 260 million years ago in Permian period, see Figure 28, and in September 2010 the first sample of polyhalite was brought to the surface. From only this source, it is estimated that there are one billion tonnes available polyhalite, making the cost of using PS low (ICL, 2022b).

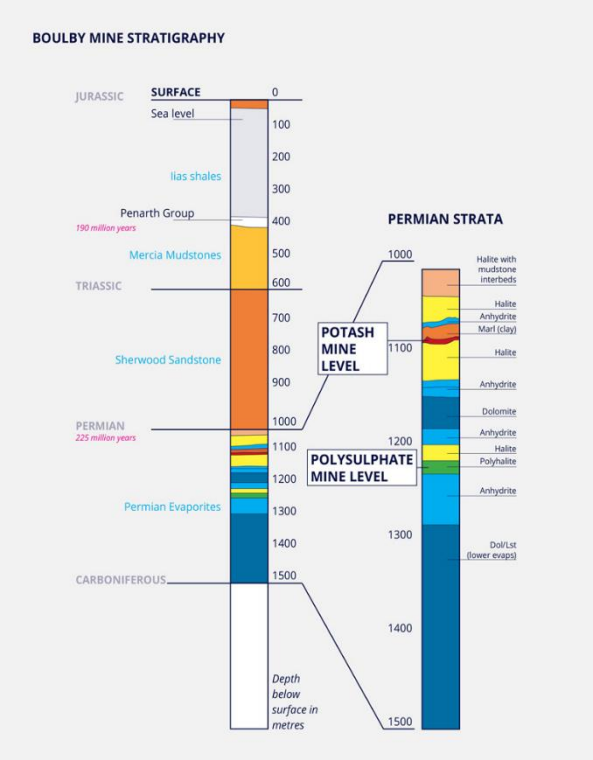

Figure 28: stratigraphy of Boulby mine where polysulphate is located in the Permian strata 1200 m below the surface level.

PS used in this project has the chemical formula $K_2Ca_2Mg(SO_4)_4 \cdot 2H_2O$ and was provided from ICL company (ICL, 2022a). The salt was slightly grey in colour and was observed to be in range from granulated to powder form. No further purification of the raw salt was performed.

4.1.4. Preparation of Brines

In this study, all brines were made artificially in the laboratory by dissolving different amounts of salts in distilled water (DW). The salts were purchased from Merck and Sigma-Aldrich. All brines were filtered with 0.22 µm milipore filter. Brine composition and properties can be found in table 3 and 4, respectively.

Valhall Formation Brine Zero Sulfate (VB0S)

The initial water saturation in chalk cores was established using a brine called VB0S. This brine represents the formation water in the chalk formation in Valhall field as it has similar composition. Valhall formation water do have a small amount of SO_4^{2-}, 1.0 mM (Puntervold, 2008), but since SO_4^{2-} is a potential determining ion that plays a major role in wettability alteration it is important to avoid SO_4^{2-} as it affects the establishment

of the core's initial wetting condition (Puntervold et al., 2007). The composition of VB0S is found in table 3.

Seawater (SW)

Seawater acts as a Smart Water in chalk due to the presence of potential determining ions Ca^{2+}, Mg^{2+} and SO_4^{2+} (Austad et al., 2008). In this study, seawater is used as a reference for Smart Water brine performance but still, seawater is the standard injection water offshore.

Seawater Polysulphate (SW-PS)

The Smart Water used in this study is seawater polysulphate (SW-PS). The brine was prepared by adding 5 g of polysulphate salt per liter SW. After stirring for 5 days the brine was filtered with 0.22 µm milipore filter and the salt residue was weighted.

Distilled Water Polysulphate (DW-PS)

To evaluate the EOR performance of polysulphate in fresh water, 5 g of PS salt was added to DW and stirred for 5 days. The brine was then filtered with 0.22 µm milipore filter and the salt residue was weighted.

Table 3: Brine composition of FW, SW, SW-PS and DW-PS

Brine	**FW (VB0S)**	**SW**	**SW-PS**	**DW-PS**
Ion	mM	mM	mM	mM
$\mathbf{Na^+}$	997.0	450.0	466.2	6.3
$\mathbf{K^+}$	5.0	10.0	28.2	17.4
$\mathbf{Ca^{2+}}$	29.0	13.0	29.6	15.2
$\mathbf{Mg^{2+}}$	8.0	45.0	47.9	5.8
$\mathbf{Cl^-}$	1066.0	525.0	528.5	9.2
$\mathbf{HCO_3^-}$	9.0	2.0	2.0	0.0
$\mathbf{SO_4^{2-}}$	0.0	24.0	55.9	31.5
Density g/cm^3	1.041	1.024	1.025	1.002
TDS g/L	62.83	33.39	38.41	5.046

Table 4: Brine properties of FW, SW, DW-PS and SW-PS

Brine	ρ (g/ cm^3)	pH (diemsionless)	$\mu_{23°C}$ (mPa·s)
FW (VB0S)	1.0416	7.3	1.02609
SW	1.0217	8.0	0.9947
DW-PS	1.0020	7.5	0.9313
SW-PS	1.0252	8.0	0.995

4.2. Analyses

Several analyses have been conducted during this study to get a broader understanding of the experimental results. In this section, a brief introduction and description of the instrument used is given.

4.2.1. PH Measurement

PH of the brines were measured using Metler Toledo SevenCompact pH meter. All measurement were conducted at room temperature. For better accuracy, the samples were measured repeatedly and the average of the three less varied values were reported with an uncertainty of $\pm$ 0.05 pH units.

4.2.2. Density Measurement

To measure the density of oil and brines, Anton Paar DMA4500 density meter was used as the measuring apparatus. The apparatus was cleaned with acetone and distilled water before each measurement. The sample was then injected with a syringe where it enters a glass u-tube allowing us to check the system for any air bubbles that disturbs the measurement.

4.2.3. Viscosity Measurement

The viscosity of the brines and the oil was determined using Anton Paar rheometer Physica MCR 302. The rheometer was cleaned with acetone and water before each measurement. Approximately 2 ml of liquid was placed on the measuring plate. The liquid was then trimmed, and gaps were filled to ensure contact between the cone-plate and the liquid. 5 measurements were conducted for each liquid when running the instrument. The instrument was run at a minimum of 3 times for each liquid and the best reproducible measurements was used to calculate the average viscosity.

4.2.4. Acid-Number (AN) and Base-Number (BN)

The amount of acid and bases of polar components (mg KOH/g) in the oils was measured by Mettler Toledo T50 auto-titrator. The method of potentiometric titration was performed in accordance with the modified versions of ASTM D664 and ASTM D2896 procedures proposed by (Fan and Buckley, 2007). All three oil solutions were measured repeatedly and the average of the three closest value was reported with an uncertainty of $\pm$ 0.05 mgKOH/g.

4.2.5. Ion Chromatography Analyses

Dionex ICS-5000+ ion chromatograph was used to analyse the anionic and cationic composition of the brines. The brine samples were prepared for the analysis by being diluted 1000 times with ultrapure Milli-Q water. The brine samples were then filtrated through 0.22 µm syringe filter. After running the analysis, the results were presented in the instruments software as peaks representing each ion detected in the solution. The concentration of each ion is related to the area of the corresponding peak. SW was used to convert each area to concentration due to the known ionic composition of SW. The following calculation were used to convert the areas:

$$\frac{C_{sw}}{A_{sw}} = \frac{C_{SO_4^{2-}}}{A_{SO_4^{2-}}} \rightarrow C_{SO_4^{2-}} = \frac{C_{sw}}{A_{sw}} \cdot A_{SO_4^{2-}} \quad (4.2)$$

Where,

C_{sw} concentration of SO_4^{2-}-ions in SW

A_{sw} area under SO_4^{2-}-peak from SW sample

$C_{SO_4^{2-}}$ concentration of SO_4^{2-} of the analysed sample

$A_{SO_4^{2-}}$ area under SO_4^{2-}-peak from the analysed sample

4.2.6. Scanning Electron Microscope and EDX

The scanning electron microscope (SEM) used to analyse the chalks surface is ZEISS SUPRA 35VP. The chalk core was crushed into pieces where the side facing outwards was placed on the stub so that the inside of the core would be analysed. Prior to the SEM analyses, the core sample was coated with a thickness of 20.0 nm palladium (Pd) using LEICA EM ACE600 sputter coater. The coating increases the electrical conductivity of the sample which increases the signal-to-noise ratio during SEM imagining that improves the quality of the images (Luyk, 2019).

To detect the elemental composition of the samples an Energy Dispersive X-ray detectors (EDX) integrated in SEM was used. The surface area to be analysed was chosen at 100x magnification and the elements was then detected and the atomic % computed by the software.

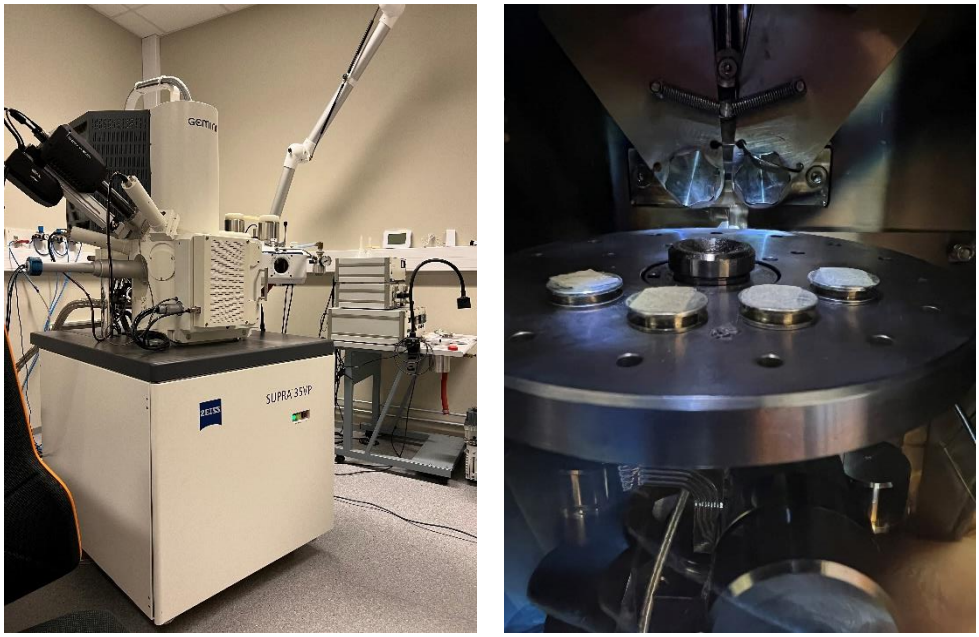

(a) (b)

Figure 29: Picture of (a) scanning electron microscope used to analyse the chalk cores and the salt residues and (b) salt residue samples inside the sputter coater during coating,

4.2.7. PHREEQC

To simulate the potential of precipitation in SW, SW-PS and DW-PS at different reservoir temperatures, a geochemical modelling program called PHREEQC was used.

4.3. Methodology

This section gives a brief description of the methods used to ensure the most optimal way of obtaining representative results. These methods have been repeatedly used and optimized during more than 20 years of experience by the EOR team at University of Stavanger. The aim of conducting these methods is to obtain conditions that are similar to the conditions found in a reservoir and thus ensuring representative results that can be compared to previous experimental work.

4.3.1. Restoration of Chalk Cores

Prior to SI experiment, all chalk cores went through a restoration process to establish S_{iw}=10 % FW and S_{oi} = 90 % oil A with AN = 0.58 mgKOH/g. The restoration process was conducted to reproduce a similar initial wetting state as in the reservoir and it consist of core cleaning, establishment of initial water saturation, oil saturation and aging.

4.3.2. Core Cleaning

Core cleaning is the first step performed in the restoration process regardless of which experiment the core will undergo. The aim of this step is to make sure that there is no salt contamination, especially SO_4^{2-}, in the core. Even though the concentration of SO_4^{2-} is small, it is enough to influence the cores initial wetting state. The core cleaning process was conducted in accordance with what is suggested by Puntervold et al., 2007. The core was placed in a Hassler core holder and flooded with 5 PVs DI-water at room temperature. The DI-water was flooded at a rate of 0.1 ml/min with a confining pressure of 20 bars. A batch test of the effluent was performed after the end of the cleaning process to ensure an effluent free of SO_4^{2-} ions. The batch was mixed with Ba^{2+} to detect for any precipitation. If precipitation occurs the water will change from being blank to cloudy, Figure 30, and we will get the following reaction:

$$Ba^{2+}(aq) + SO_4^{2-}(aq) \leftrightarrow BaSO_4(s) \quad (4.3)$$

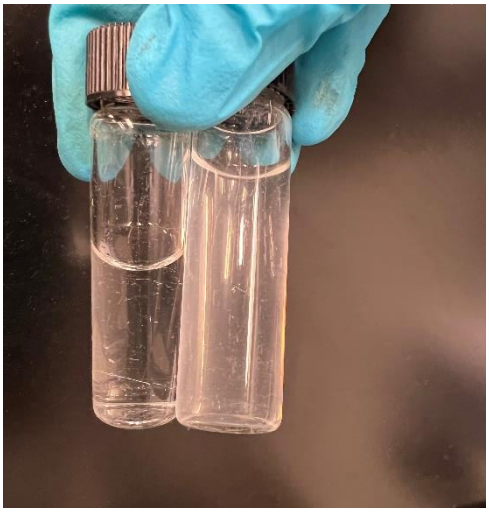

Figure 30: Batch test showing a blank sample (left) with no precipitation of $BaSO_4$ and a cloudy sample (right) indicating precipitation of $BaSO_4$.

4.3.2.1. Permeability and Porosity Calculation

The data used to calculate permeability was collected during the core cleaning process at room temperature. The average pressure drop, ΔP, were measured at three different flooding rates; 0.05, 0.1 and 0.15 ml/min. Knowing the cores length, L, diameter, D, and the viscosity, μ, of DI-water, the permeability was then calculated using Darcy's equation for each rate and its corresponding pressure drop. The average permeability from these three rates was then reported.

$$k = \frac{q}{\Delta P} \cdot \frac{\mu \cdot L}{A} \tag{4.4}$$

Porosity calculation was conducted during the establishment of initial water saturation. After cleaning, the chalk core was then dried in an oven at 90°C until reaching a stable dry weight, W_{dry}. The core was then fully saturated with diluted FW and the saturated weight, W_{sat} was noted. Since the core length and diameter are known, the bulk volume, V_b, can be calculated as follows:

$$V_b = L \cdot \frac{\pi \cdot D^2}{4} \tag{4.5}$$

The density of the diluted FW was measured and the pore volume, V_p, was found by:

$$V_p = \frac{W_{sat} - W_{dry}}{\rho_{diluted\ FW}} \tag{4.6}$$

Then the porosity, φ, was calculated:

$$\varphi = \frac{V_p}{V_b} \tag{4.7}$$

4.3.2.2. Establishment of initial water saturation

Completely dry cores were fully saturated with 10 times diluted FW so that the concentration of the obtained 10% initial water saturation is the same as the undiluted FW which corresponds to VB0S given in table 3. Prior to saturation with diluted FW, the dry weight of the core was measured. The core was then placed in a cylindrical plastic container with marbles to minimize the contact area between the core and the container enabling the water to freely saturate the pores. The container with the core was then placed in a desiccator under vacuum, Figure 33, before the diluted FW was slowly introduced to the core until it was completely covered. To enable all the pores to be saturated, the core was held under vacuum with diluted FW for 30 minutes. The weight of the fully saturated core was measured and the target weight, W_{target}, that represents the weight of the core with S_{iw}=10 % FW is calculated as follows:

$$W_{target} = W_{dry} + V_p \cdot S_{iw} \cdot \rho_{diluted\ FW} \tag{4.8}$$

The core was then placed in a desiccator with silica gel to adsorb the evaporated water until the W_{target} is reached. It was then placed in a container for at least 3 days to enable an even distribution of the remaining FW.

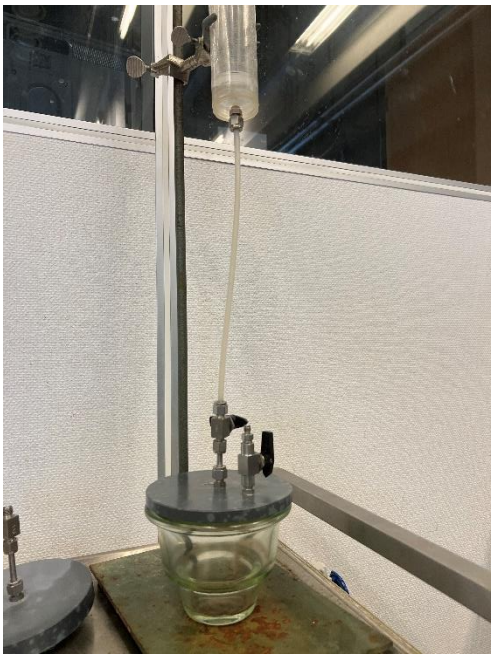

Figure 31: Setup for establishing initial water saturation used in the laboratory.

4.3.2.3. Establishment of Initial Oil Saturation

After establishing S_{iw}=10 % FW the core was then placed in a Hassler core holder to saturate the remaining pores with oil. The oil saturation setup was mounted in an oven where oil flooding was conducted at 50°C, to lower the pressure drop across the core, with a confining pressure of 15 bars. To ensure a full saturation of the remaining pores, the air in the core holder was removed by vacuuming for 10 minutes. The core was then injected at a rate of 0.5 ml/min with 1 PV of oil from both sides simultaneously and flooded with 1.5 PV of oil at a rate of 0.2 ml/min in each direction. The effluent oil was collected to be used in the next restoration step, aging.

4.3.2.4. Ageing

After saturating the remaining pores with oil, the core was then taken out of the core holder and wrapped with Teflon, Figure 32, to ensure no unrepresentative adsorption of oil on the external surface. The core was then placed in an ageing cell with marbles and covered completely with the effluent oil from the oil saturation process. The cell was then placed in an oven at 90°C for two weeks. After two weeks of ageing, the core was then taken out, unwrapped and the final weight was measured. Finally, the core is now ready for the main experiment; spontaneous imbibition.

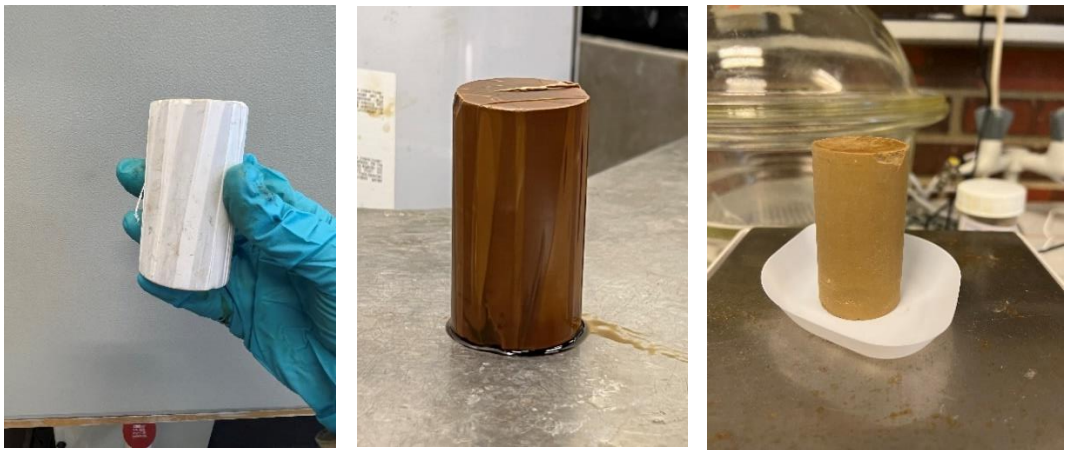

(a) (b) (c)

Figure 32: Picture (a) shows the core wrapped in Teflon prior to ageing, while (b) shows the core after aging and (c) is the core right before spontaneous imbibition test.

4.3.3. Oil Recovery by Spontaneous Imbibition

Once the core has gone through the restoration process it mimics the reservoir condition more and is ready to undergo a spontaneous imbibition test. The core was placed in an imbibition stainless-steel cell with marbles to increase the surface area for imbibition, see Figure 33 for illustration. The cell with the core were then filled with imbibition brine. For the SI test conducted at 110°C, the imbibition brines used for SK1, SK2, SK3, SK4 are FW, SW, DW-PS and SW-PS, respectively. SI test conducted at 90°C used the cores SK5, SK6, SK7 and SK8 with FW, SW, DW-PS and SW-PS, respectively, as the imbibition brines. The cells were then placed in the oven and connected to a piston cell that contains the same imbibition brine providing 10 bars to avoid any water evaporation. A burette was used to collect the recovered oil at the outlet.

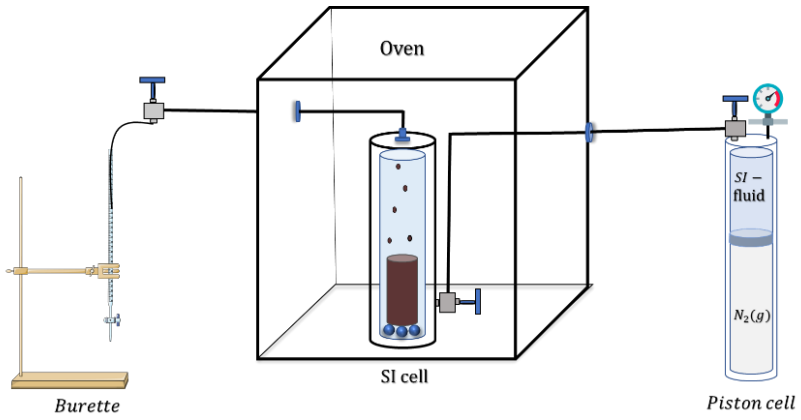

Figure 33: Setup used for spontaneous imbibition.

5. Results and Discussion

In this chapter results obtained from the experimental work are presented and further discussed. Analysis obtained from SEM, EDX and ion chromatography are presented and used to get a broader understanding behind the results achieved from spontaneous imbibition test. Stability of PS brines at different temperatures is evaluated both by simulation using PHREEQC and observing during SI test. Finally, SI test of PS brines are presented at two different temperatures and compared with SW and FW. The results are then discussed.

5.1. Scanning Electron Microscope Analysis with EDX

The outcrop chalk material used in this thesis was studied by SEM to investigate the heterogeneity of the core as well to confirm that the core is biogenic, a result of biological processes which is mentioned in chapter (3.1.1). The composition of the core is also analysed to confirm the chalk purity. The residue of the Smart Water brines DW-PS and SW-PS was also studied by SEM to investigate the undissolved salt composition. The analysis results are presented in the following subchapters.

5.1.1. SEM Analysis of Chalk Outcrop Core

To study the pores and grains of the chalk material SEM analysis was performed of the uncleaned Stevns Klint chalk outcrop. With this method images of the material were obtained, as well as an average composition of the chalk surface. This information is important as it confirms that the material used in this study is a biogenic chalk material consisting of mostly $CaCO_3$ and with heterogeneous porosity.

Figure 34 shows a SEM image captured at 100x magnification The image gives an overview of how heterogenous the chalk surface is. The porous space can also be observed by the dark spots in the image.

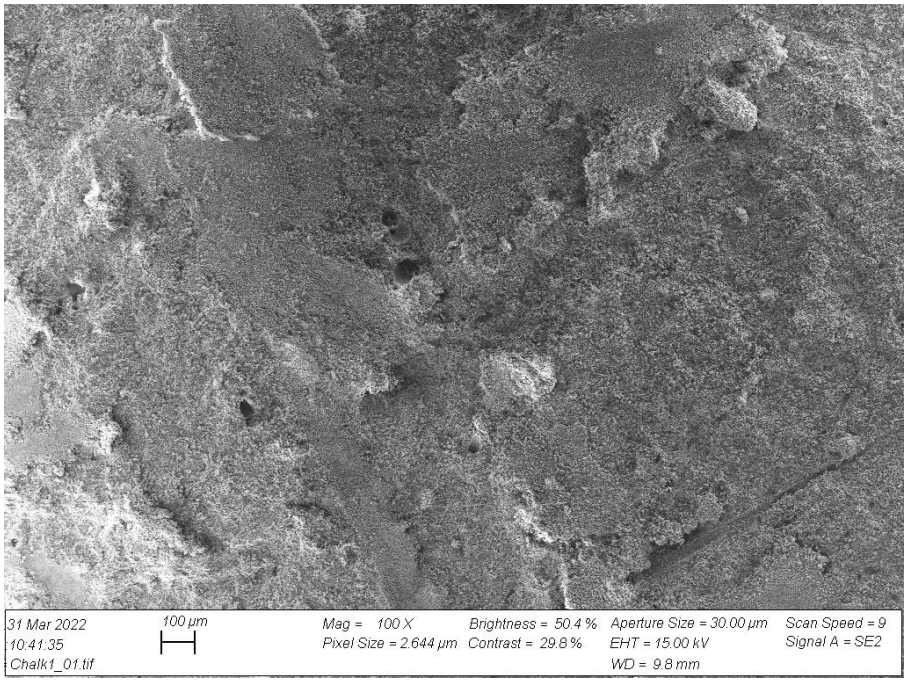

Figure 34: SEM image of the uncleaned Stevns Klint outcrop chalk core at 100x magnification.

The EDX analysis was performed on the same surface area shown in Figure 34. The results obtained are presented in table 5 below.

Table 5: Elemantal composition of the uncleaned Stevns Klint outcrop chalk core

Element	Weight %	Atomic %
Na	0.01	0.02
Mg	0.08	0.13
Al	0.13	0.19
Si	0.57	0.81
S	0.44	0.54
K	0.22	0.23
Ca	98.54	98.06

The elemental composition in table 5 indicates a very pure calcite ($CaCO_3$) surface with atomic % of 98.06 calcium (Ca). The element S is also detected but with a small atomic % of 0.54 and is most probably related to both the amount of SO_4^{2-}-ions and anhydrite ($CaSO_4$ (s)). The Mg detected on the surface might be due to the presence of $MgCO_3$ but can also indicate clay content when combined with the detected Al and Si. With an atomic % of 0.19 and 0.81 for Al and Si, respectively, the amount of clay present on the

chalk surface is very small. To analyse the chalk surface further, the chalk sample was scanned at 10 000x magnification presented in Figure 35.

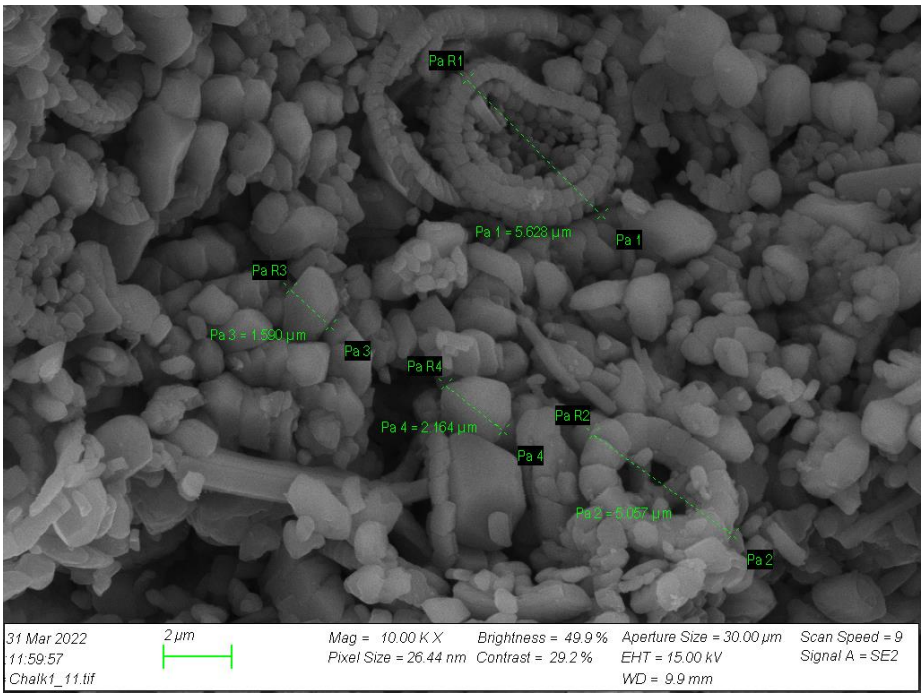

Figure 35: SEM image of the uncleaned Stevens Klint outcrop chalk core at 10 000 x magnification.

The heterogeneity of the chalk surface is more clearly observed after increasing the magnification significantly. A lot of small grains with a diameter of ~ 2 µm are observed along with some large coccoliths with a diameter of ~ 5 µm. The dark spots observed in the image presents the pores of the chalk with varying size ranging from 0.5- 3 µm.

5.1.2. SEM of Polysulphate Salt Residue

The salt residue collected during filtering of the PS brines was analysed by SEM and EDX to investigate the average ion composition and how the salt particles are shaped and their size. Since Smart Water is based on the ionic composition it is important to have an overview of which ions are not dissolved. SEM image captured of DW-PS brine sample at 1000x magnification is presented in Figure 36 below.

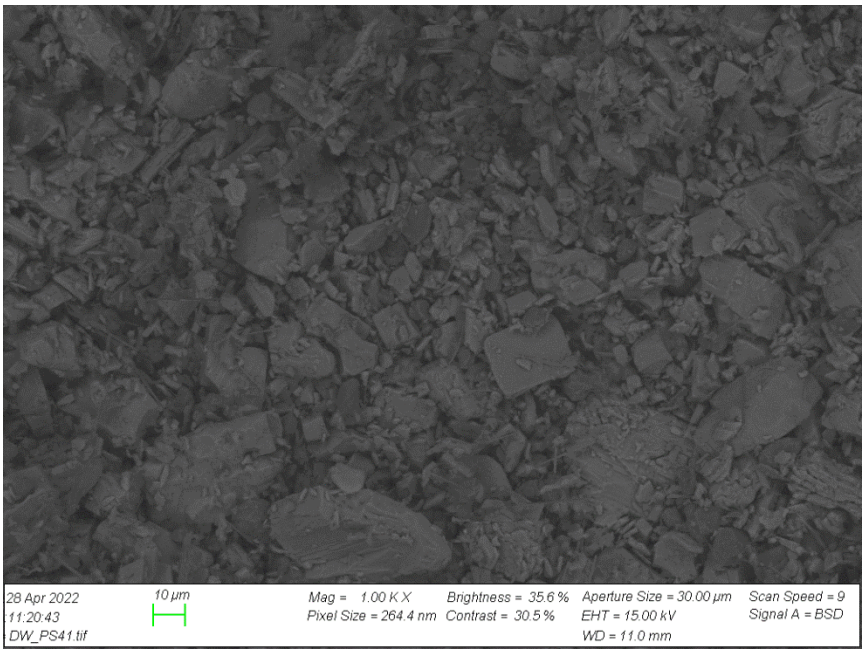

Figure 36: SEM image of the salt residue from DW-PS at 1000 x magnification

It appears that the size of the salt particles in the residue varies a lot with size ranging from 0.2 µm up to 30 µm. The smallest particles are observed to be attached on the big particles. When magnifying the scanned area, the variation in shapes of the salt particles become more obvious in Figure 37 below.

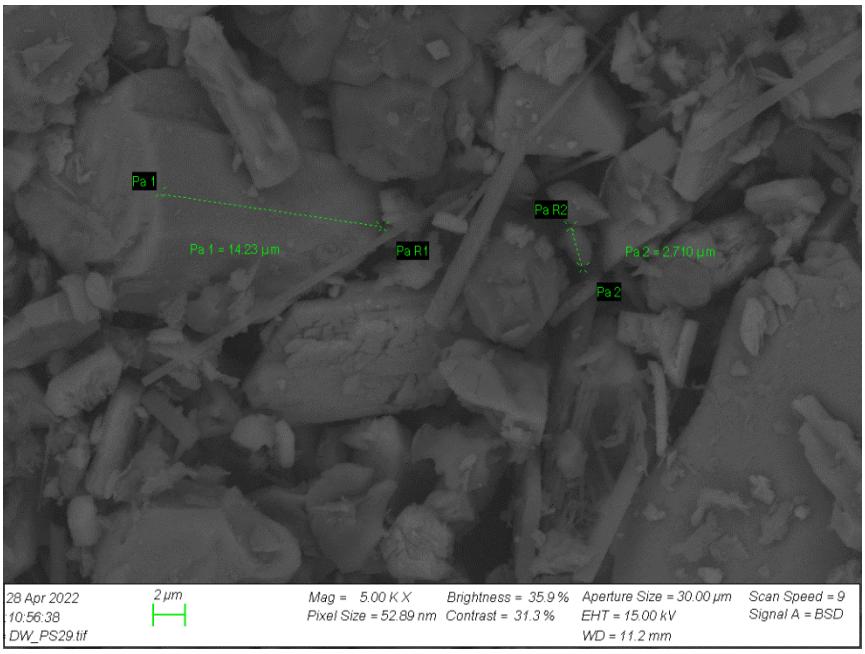

Figure 37: SEM image of the salt residue from DW-PS at 5000 x magnification

Big cylindrical-like particle shapes along with some thin elongated particles is observed in the image. An EDX analysis was performed to study the elemental composition of the salt residue. The results are given in table 6.

Table 6: Elemental composition of the salt residue from DW-PS brine

Element	Weight %	Atomic %
Na	4.77	7.0
Mg	8.46	11.74
Al	0.32	0.4
Si	3.59	4.32
S	31.92	33.61
K	0.61	0.53
Ca	50.33	42.4

Almost 88 atomic % of the salt residue from DW-PS brine consist of the elements Ca and S and Mg. These three elements are the key elements in wettability alteration process and were clearly not dissolved completely when the polysulphate salt was mixed with distilled water.

Salt residue from SW-PS brine was also analysed using SEM. Figure 38 shows SEM image captured at 1000x magnification of the salt residue.

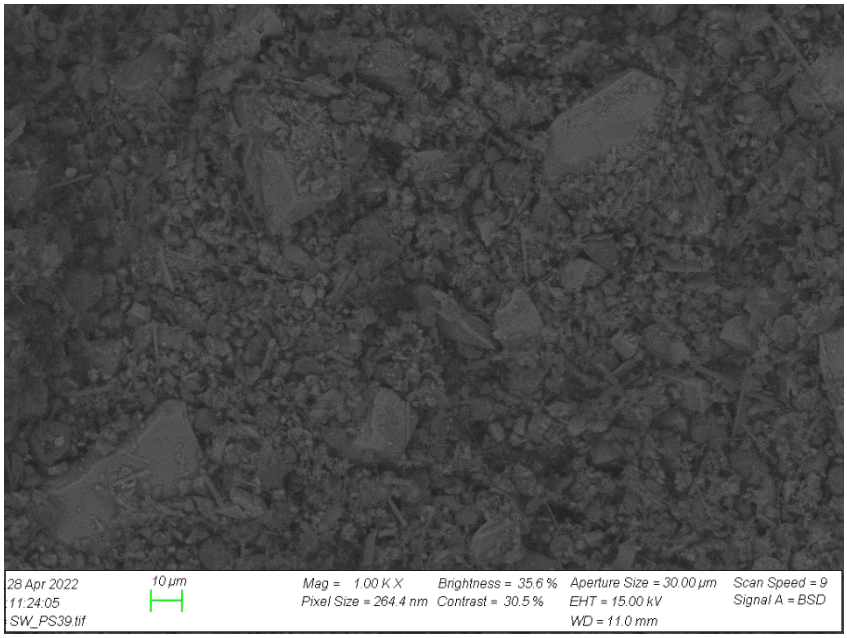

Figure 38: SEM image of the salt residue from SW-PS at 1000 x magnification

The residue from SW-PS is observed to be dominated with small particles. Some big particles that can be up to 40 µm are also observable. The sample was also scanned at 5000x magnification to get a closer look at the residue. Figure 39.

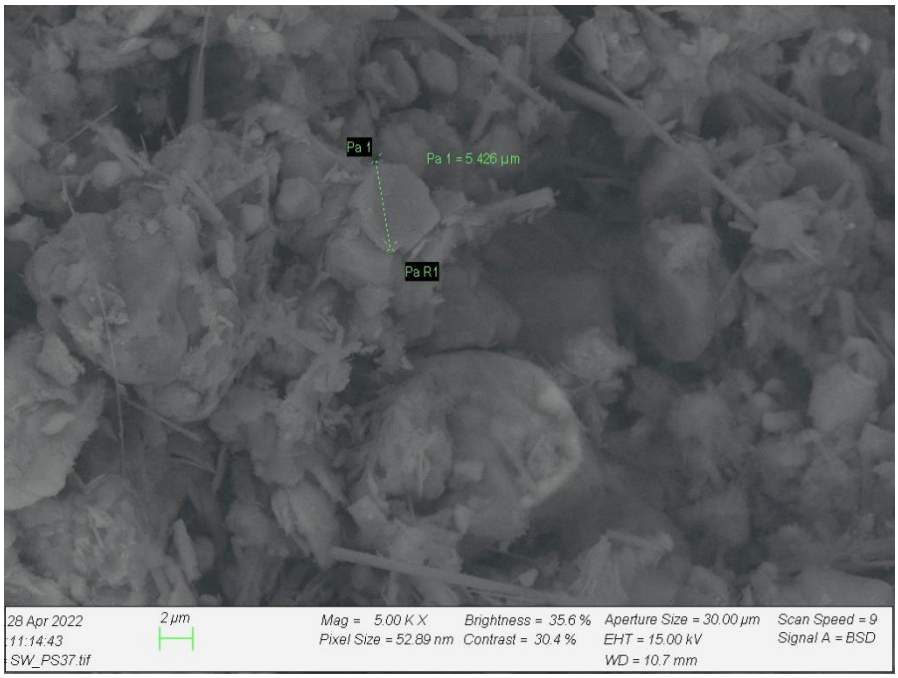

Figure 39: SEM image of the salt residue from SW-PS at 5000 x magnification

Some big particles that are mainly covered by small particles are observed in the SEM image. The elongated particles found in Figure 39 is also observed here. To analyse the elemental composition of the salt residue sample, an EDX analysis was performed with the results presented in table 7.

Table 7: Elemental composition of the salt residue from SW-PS brine

Element	Weight %	Atomic %
Na	6.96	8.83
Mg	32.16	38.61
Al	1.66	1.80
Si	14.4	14.96
S	17.11	15.58
K	1.74	1.3
Ca	25.98	18.92

The elements Ca and S have a much lower atomic% compared to DW-PS salt residue with 18.92 and 15.58 atomic% respectively. The element with the highest atomic% is Mg with 38.61 atomic%. From the elemental composition it appears that much more calcium and sulphate have been dissolved in SW-PS brine, but magnesium has dissolved less. From table 7, the concentration of Mg^{2+} in SW relatively high compared to the concentration of the other two determining ions, Ca^{2+} and SO_4^{2-}. This may indicate that SW is already saturated with Mg^{2+} so when PS was introduced not all the Mg^{2+} dissolved due to oversaturation.

5.2. Results of Ion Chromatography Analysis

When PS was added to DW and SW the composition of these two brines changed and became unknown. In order to study the ion composition of the prepared PS brines, IC analyses was used. Ion composition in Smart Water is very crucial when it comes to wettability alteration. It is therefore important to investigate the ion composition and focus especially on potential determining ions as these are the key parameter to alter wettability. The PS brines were IC analysed along with SW and DW (fresh water). The results obtained are presented in Figure 40 below.

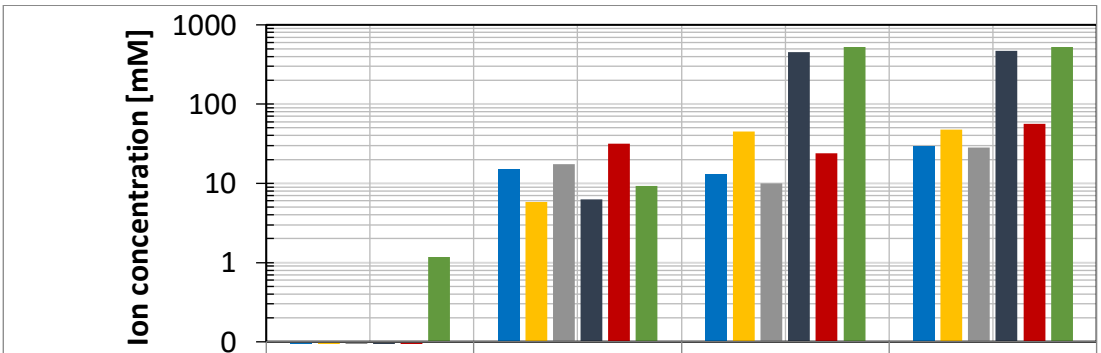

	DW	DW-PS	SW	SW-PS
Calcium (Mm)	0.0	15.2	13.0	29.6
Magnesium (Mm)	0.0	5.8	45.0	47.9
potassium (Mm)	0.0	17.4	10.0	28.2
Sodium (Mm)	0.0	6.3	450.0	466.2
Sulphate (Mm)	0.1	31.5	24.0	55.9
Chloride (Mm)	1.2	9.2	525.0	528.5

Figure 40: Ion composition obtained by ion chromatography analyses of DW, DW-PS, SW, and SW-PS.

The histogram in Figure 40 shows the ion composition in each brine. DW which is used as the freshwater in this study has a very low amount of sulphate and chloride with a concentration of 0.1 and 1.2 mM, respectively. Otherwise, there were no other ions present in DW. When adding 5.0 g of polysulphate per litre freshwater the concentration of all the ions provided by PS start to rise. The ion concentration of SW was already known. The IC analyses only confirms the ion composition of SW that is presented in table 8. The change in the ion composition when adding 5.0 g of polysulphate to 1 litre of SW is not as significant as when adding PS to freshwater. The concentration of ions provided by PS are listed in table 8 below:

Table 8: Concentration of ions provided by polysulphate salt to DW-PS and SW-PS

	Ca^{2+} [mM]	Mg^{2+} [mM]	K^{+} [mM]	Na^{+} [mM]	SO_4^{2-} [mM]	Cl^{-} [mM]
DW-PS	15.2	5.8	17.4	6.3	31.4	8.0
SW-PS	16.6	2.9	18.2	16.2	31.9	3.5

The concentration of Ca^{2+} , Mg^{2+} , K^{+} , SO_4^{2-}, $Na^{+}$and Cl^{-} was raised with 15.2, 5.8, 17.4, 6.3, 31.4 and 8.0 mM, respectively, when PS was added to DW. The same ions were also increased in concentration when PS was added to SW. The only two ions that did not increase with similar concentration as in DW-PS are Mg^{2+} and Cl^{-}. This is probably due to the high saturation of these two ions in SW that the brine was only capable to take dissolve a less amount of these two ions.

The most important ions in wettability alteration are the three potential determining ions, Mg^{2+}, Ca^{2+} and SO_4^{2-}. The concentration of these three ions in DW, DW-PS, SW and SW-PS are presented in Figure 41.

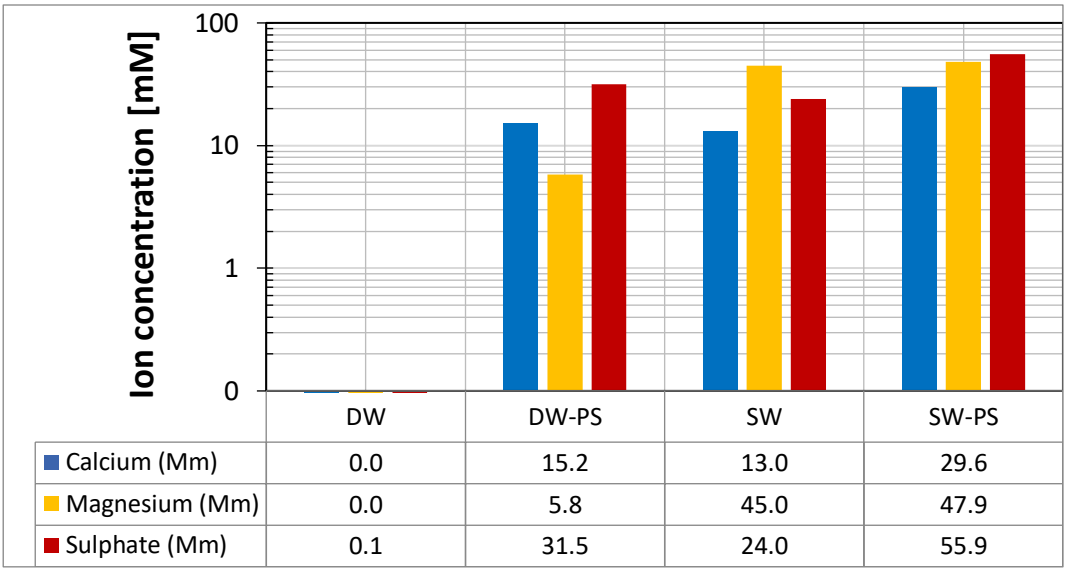

Figure 41: Ion composition of the potential determining ions (Ca^{2+}), (Mg^{2+}), and (SO_4^{2-}) in DW, DW-PS, SW, and SW-PS.

The concentration of the determining ions is absent in DW, except of sulphate with a very low concentration of 0.1 mM. Using DW as a Smart Water will most probably not contribute to enhance the oil recovery as it misses the ions that triggers the wettability alteration in carbonates. When adding PS to DW it provides DW with potential determining ions. Compared to SW, the concentration of Ca^{2+} and SO_4^{2-} in DW-PS is higher with 15.2 and 31.5 mM. Although the concentration of these two ions is higher, Mg^{2+} in DW-PS is almost 8 times lower with 5.8 Mm. In SW-PS the concentration of Ca^{2+} and SO_4^{2-} are more than 2 times higher than the concentration in SW with 29.6 and 55.9 mM. The concentration of Mg^{2+} in SW-PS has not increased with the same level as the other two ions. As discussed, this is due to the brine being oversaturated with Mg^{2+}.

Based on the ion concentration, PS brines shows a potential of inducing wettability alteration as they contain a decent amount of the potential determining ions. Since the brines will be tested for oil recovery at high temperatures, 90°C and 110°C. It would be useful to get an idea of how stable the brines are by simulation.

5.3. PHREEQC – Simulation Results

To evaluate the stability of PS brines at high temperature simulation by using PHREEQC was used. The simulation results give us valuable information about which minerals are likely to precipitate at which temperature. By gaining the information about which ions are precipitating we can further understand the PS brines performance during the SI experiments.

SW, SW-PS and DW-PS ion compositions was simulated at different temperatures and the same pressure condition as when performing spontaneous imbibition test which is 10 bar. The results are presented as saturation index vs temperature. The saturation index tells us how possible some minerals will precipitate based on the given ion composition and temperatures. Three minerals sowed potential for precipitating in SW, SW-PS and DW-PS. The results are presented Figure 42, 43 and 44, respectively.

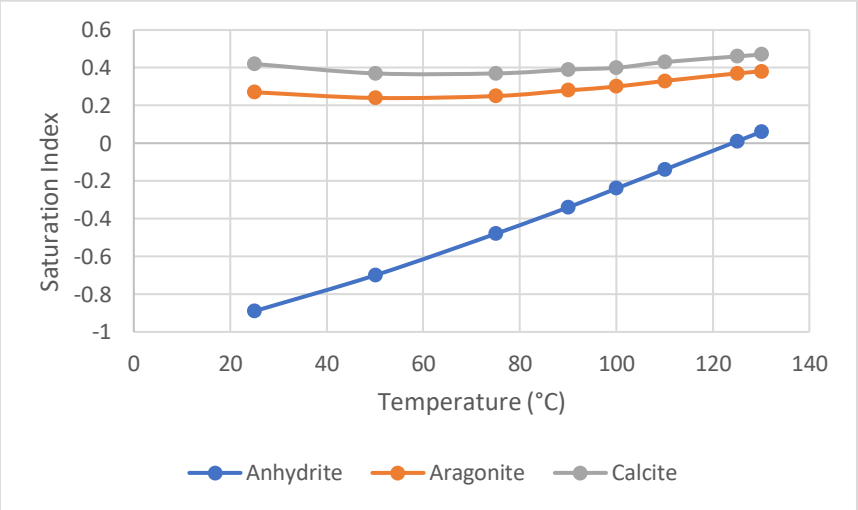

Figure 42: Saturation index vs temperature of SW

Saturation index below 0 means that the mineral in the brine is undersaturated, saturation index = 0 indicates saturated and above 0 is oversaturated with potential of precipitating. When the temperature increases the saturation index of anhydrite ($CaSO_4$) increase from -0.89 to 0.06 in SW. The potential of anhydrite precipitation increases at a high rate compared to aragonite ($CaCO_3$) and calcite ($CaCO_3$). The saturation index becomes positive just below 120°C indicating oversaturation that might result in precipitation. The highest temperature that SW will be exposed to in this study is 110°C. The

saturation index of anhydrite at this temperature is -0.14 indicating no potential of precipitation.

Aragonite and calcite have positive but an overall stable saturation index that increase slightly with increasing temperature. The highest saturation index is 0.38 and 0.47, respectively, at 130°C. This means that the potential of $CaCO_3$ being precipitated is always there. Just because a mineral is oversaturated with positive saturation index does not mean that it would precipitate in real world but rather tell us the potential of the mineral precipitating. Simulation of saturation index vs temperature of SW-PS is presented in Figure 43 below.

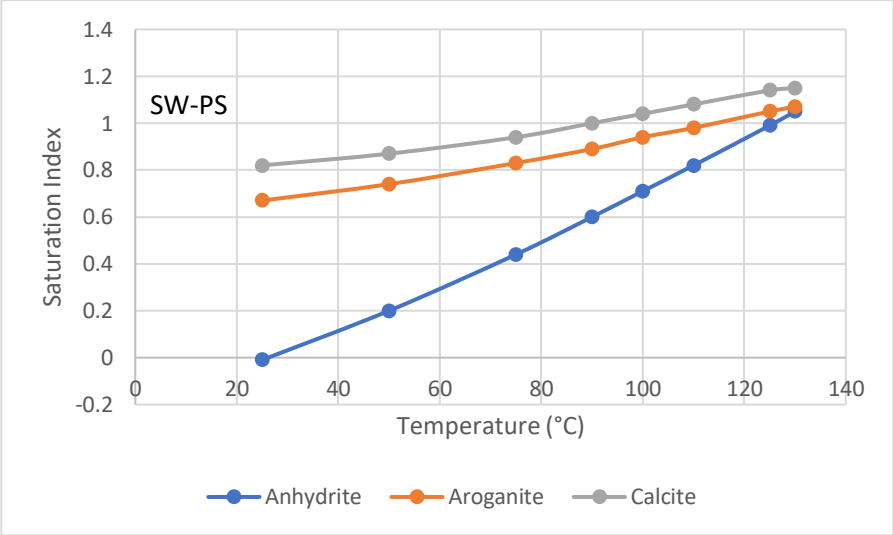

Figure 43: Saturation index vs temperature of SW-PS

Already at 25°C the saturation index of anhydrite is 0 meaning that the mineral in SW-PS brine is saturated. The saturation index increases with temperature until reaching the last simulated temperature step of 130°C with a saturation index of 1.07. At 90°C and 110°C, which is the temperatures the brine will be exposed to in this study, the saturation index of anhydrite is 0.6 and 0.82, respectively. There are potential of anhydrite precipitating during the experiments. The results for DW-PS are presented in Figure 44.

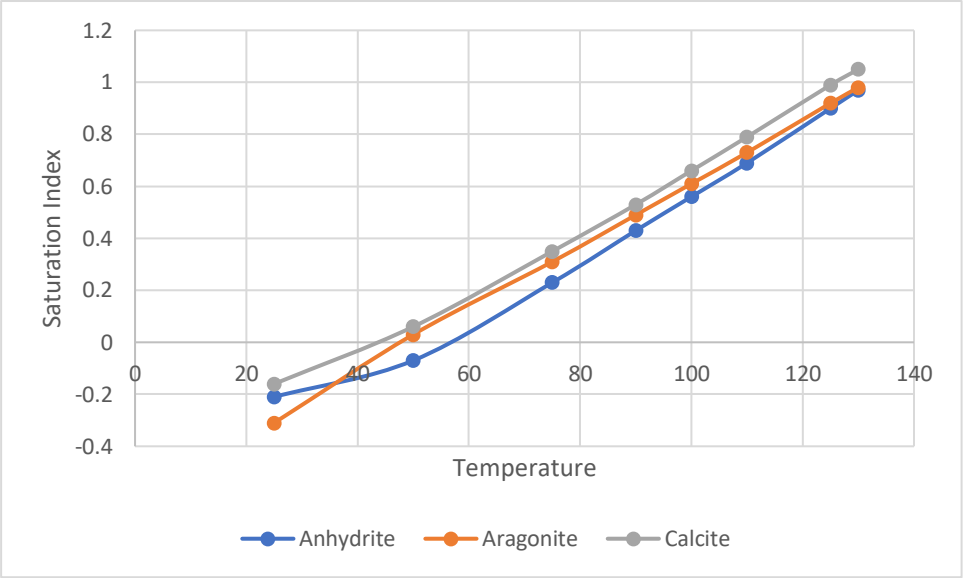

Figure 44*:* Saturation index vs temperature of DW-PS

All three minerals increase linearly with temperature in DW-PS. The saturation index switches from negative to positive at approximately 50°C for all three minerals meaning that the potential of getting precipitation occurs at a much lower temperature than the test temperature used in this thesis. The saturation index in DW-PS is a little bit lower at 90°C and 110°C compared to the saturation index in SW-PS at the same temperatures. The potential of getting precipitation is there but it is less than SW-PS. No precipitation was observed when running spontaneous imbibition with DW-PS at 90°C and 110°C.

Aragonite and calcite in SW-PS have higher saturation index at 25°C than in SW at 130°C. The saturation index for both minerals increased with temperature. At 90°C the saturation index for aragonite and calcite are 0.89 and 1.0, respectively, and increases to 0.98 and 1.08 at 110°C. The result from the simulation concludes that there is much higher potential of having precipitation of the three presented minerals in SW-PS than in SW. Both brines underwent a spontaneous imbibition test at 90°C and 110°C where they were checked for any precipitation during the experiment in addition to evaluate the recovery performance of these two brines.

5.4. Spontaneous Imbibition

In this section the results obtained from the spontaneous imbibition test are presented and discussed. The main objective of this experimental work is to test whether the PS salt induces wettability alteration and if so, how good is the effect. Spontaneous imbibition is used as the test method due to its ability to measure and quantify wettability. The test was performed at two different temperatures, 90 °C and 110°C, and a of total 8 Stevens Klint cores was restored through cleaning, establishment of 10% FW saturation and 90% of Oil A and aging for two weeks before performing the test. Four imbibing brines was tested at each temperature, FW, SW, and the smart waters DW-PS and SW-PS. The test was run until reaching a minimum of 5 days of plateau (no oil production).

5.4.1. Spontaneous Imbibition at 110°C

Spontaneous imbibition at 110°C was performed using chalk cores SK1, SK2, SK3, and SK4 with the imbibing brines FW, SW and the smart waters, DW-PS and SW-PS, respectively. The test was carried out in a cell with 10 bar backpressures to avoid the water from evaporating.

Spontaneous imbibition of FW

Oil recovery by spontaneous imbibition with FW as the imbibing brine was set as the reference test since the initial saturation of all cores are established with FW. The results obtained from performing SI of FW at 110°C is represented in Figure 45 below where the oil recovery (OOIP %) is plotted against time (days).

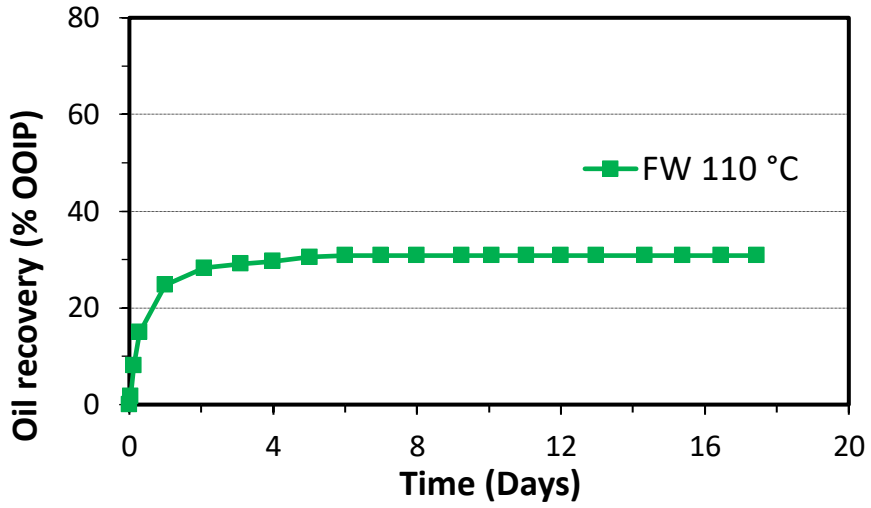

Figure 45: Spontaneous imbibition at 110°C of formation water into SK1 outcrop chalk core saturated with oil A with AN = 0.58 mgKOH/g

The oil production is rapidly increasing the first two days. After day two, less and less oil was produced until day 6 where the production plateau was reached resulting in an oil recovery of 30.8% of the OOIP. The oil produced from the first 1-3 hours is a result of thermal expansion of the oil. The oil produced after thermal expansion is mainly related to capillary forces and the initial wetting state of the chalk rock. Since the potential determining ion SO_4^{2-} is not present in the formation water there are no wettability alteration taking place to produce oil.

Spontaneous imbibition of SW

SI profile of SW are represented in the Figure 46 below. The same trend is observed with SW where the first 1-3 hours the recovered oil is a result of thermal expansion. Since the potential determining ions are present in the brine. The oil produced after that is mainly related to capillary forces along with the initial wetting of the core and wettability alteration due the presence of SO_4^{2-}. After 24 hours the oil recovery exceeds the oil recovery obtained by FW. The production reaches the plateau after 12 days with 49.7% recovered oil.

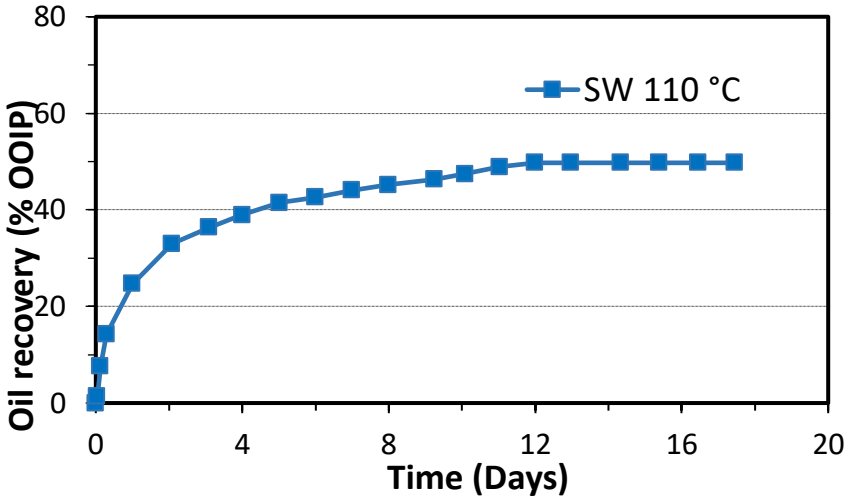

Figure 46: Spontaneous imbibition at 110°C of seawater into SK2 outcrop chalk core saturated with 10% FW and 90% oil A with AN = 0.58 mgKOH/g

Spontaneous imbibition of DW-PS

The results obtained by spontaneously imbibing distilled water with polysulphate is presented in Figure 47. The same trend is observed compared to SW where the first 1-3 hours of produced oil comes from thermal expansion. Since PS salt contains SO_4^{2-} it will trigger an alteration in wettability. After 24 hours the oil recovery is beyond of what is obtained by FW as the imbibing brine. The produced oil after thermal expansion is a result of a combination of capillary forces and wettability alteration. The SI profile reaches the plateau after 24 days with 48.4 % oil recovered.

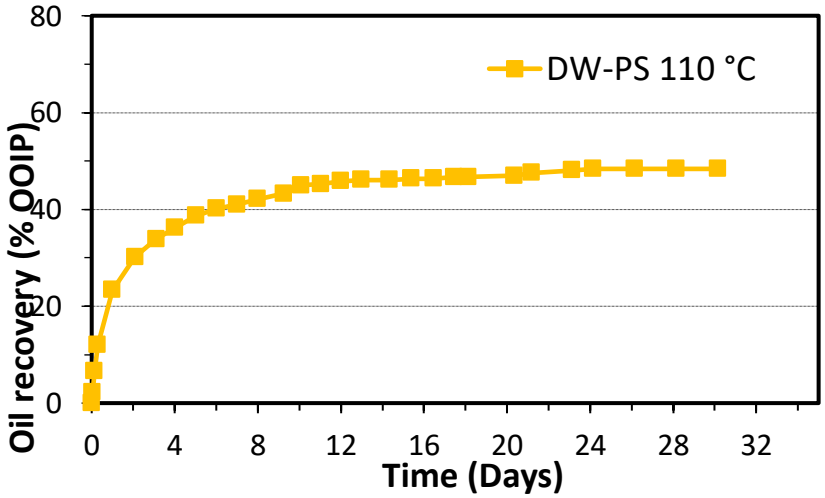

Figure 47: Spontaneous imbibition at 110°C of destilled water with polysulphate into SK3 outcrop chalk core saturated with 10% FW and 90% oil A with AN = 0.58 mgKOH/g

Spontaneous imbibition of SW-PS

Last SI at 110°C test was conducted with the brine seawater with polysulphate, Figure 48. The SI profile obtained is similar to the two other sulfate-containing brines, SW and DW-PS. The SI profile increases rapidly during the first 24 hours before it starts to decrease. The first 1-3 hours is produced oil influenced by thermal expansion. Then capillary forces and wettability alteration become the main driven parameters in producing oil.

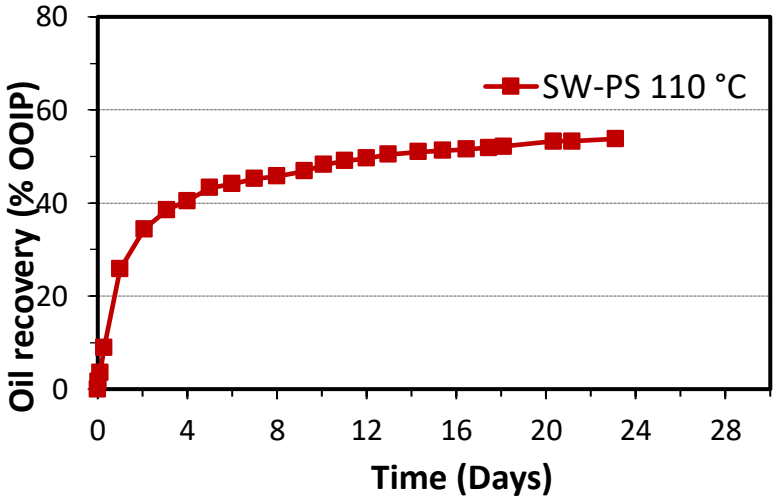

Figure 48: Spontaneous imbibition at 110°C of seawater with polysulphate into SK4 outcrop chalk core saturated with 10% FW and 90% oil A with AN = 0.58 mgKOH/g

The plateau was not reached for this experiment as the inlet line was clogged due to precipitation. This prevented the brine from flowing into the cell during each measurement and the pressure truly dropped which made the water evaporate. No precipitation was detected on the outlet line. However, the total produced oil after 24 days was 53.8% of OOIP.

5.4.2. Spontaneous Imbibition at 90°C

Spontaneous imbibition was also performed below the waters boiling point at 90°C. The chalk cores used for this experiment was SK5, SK6, SK7, and SK8 with the imbibing brines FW, SW and the smart waters, DW-PS and SW-PS, respectively. The SI test was conducted under same pressure conditions as the test performed at 110°C with 10 bars backpressures avoiding the water from evaporating.

Spontaneous imbibition of FW

SI test was conducted with formation water as the imbibing brine, Figure 49. The SI profile follows the same trend as seen with FW at 110°C. Thermal expansion drives the oil out of the core the first 1-3 hours. Then the oil production is mainly driven by capillary forces and the chalk initial wetting state. No wettability alteration is induced due to lack of SO_4^{2-}.After 12 days of production the plateau was reached with 21.8% recovered oil.

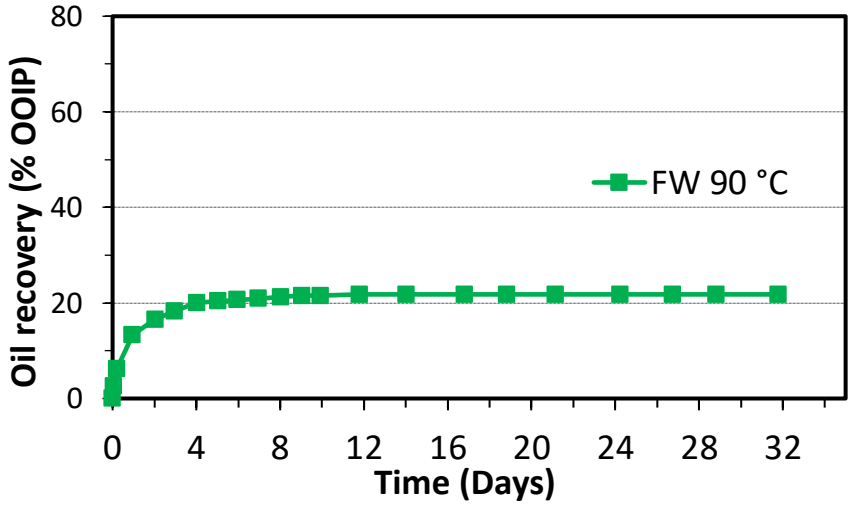

Figure 49: Spontaneous imbibition at 90°C of formation water into SK5 outcrop chalk core saturated with 10% FW and 90% oil A with AN = 0.58 mgKOH/g

Spontaneous imbibition of SW

The results obtained from spontaneous imbibition of SW at 90°C is shown in Figure 50 below. The SI profile of SW follows the same trend as FW in Figure 49 above. Th first oil produced is a consequence of thermal expansion. In addition to capillary forces the SW brine contain SO_4^{2-} that induces wettability alteration. The production plateau is reached after 21 days with 36.8 % recovery of OOIP.

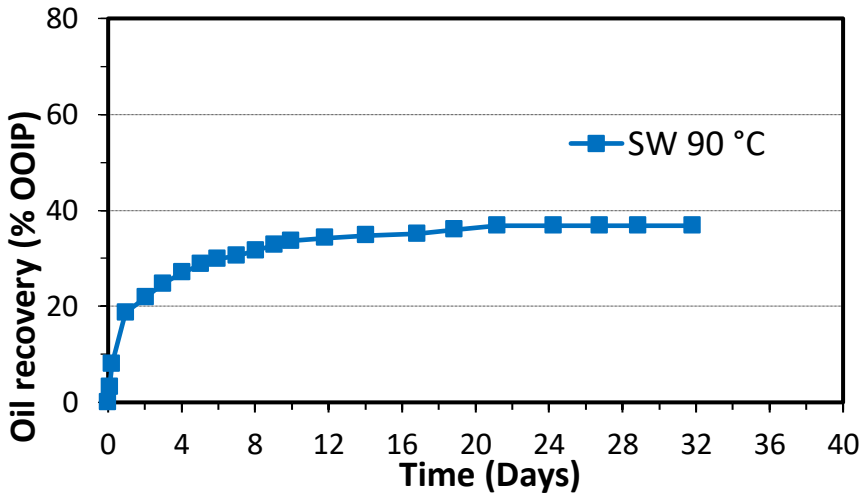

Figure 50: Spontaneous imbibition at 90°C of seawater into SK6 outcrop chalk core saturated with 10% FW and 90% oil A with AN = 0.58 mgKOH/g

Spontaneous imbibition of DW-PS

Distilled water with polysulphate was imbibed spontaneously into chalk core SK7. The oil recovery vs time of this SI experiment is presented in Figure 51. Still thermal expansion is the driven force of the first oils produced. Due to the presence of SO_4^{2-} in PS salt, the brine will induce wettability alteration that acts along with capillary forces. The total amount of oil produced is 35.2 % of OOIP. The plateau was reached after 29 days.

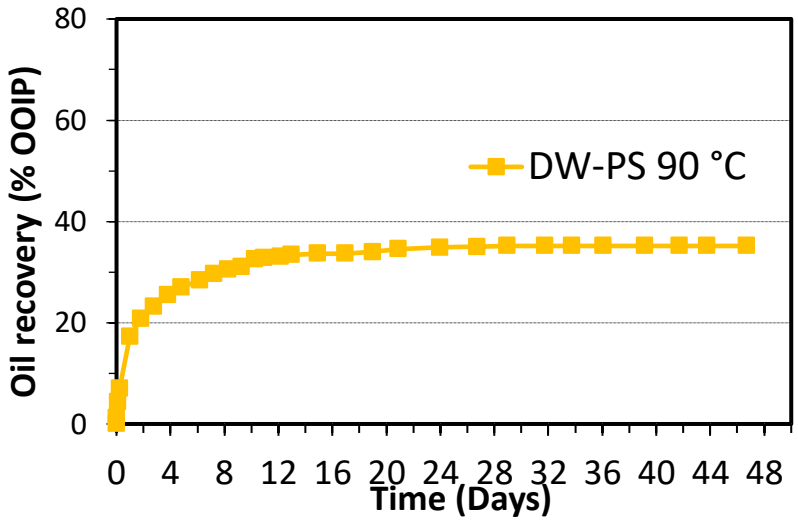

Figure 51: Spontaneous imbibition at 90°C of destilled water with polysulphate into SK7 outcrop chalk core saturated with 10% FW and 90% oil A with AN = 0.58 mgKOH/g

Spontaneous imbibition of SW-PS

Same trend is obtained by spontaneously imbibing seawater with polysulphate, Figure 52. The first force acting is the thermal expansion of the oil which is taken over by capillary forces and wettability alteration due to the presence of SO_4^{2-}.Total amount produced is 44.8% after 43 days.

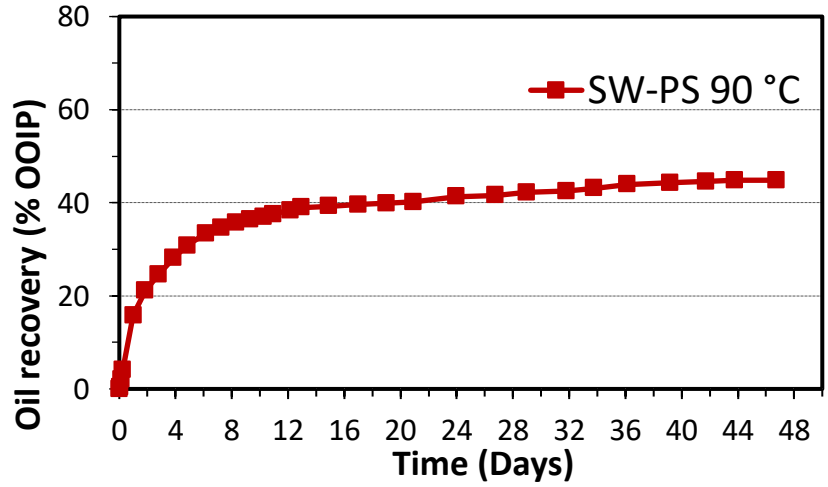

Figure 52: Spontaneous imbibition at 90°C of seawater with polysulphate into SK8 outcrop chalk core saturated with 10% FW and 90% oil A with AN = 0.58 mgKOH/g

5.5. Spontaneous Imbibition – Discussion

5.5.1. Temperature Effect

To see and evaluate whether temperature influences the wettability alteration in chalk cores, the results obtained by spontaneous imbibition with the same brine at different temperatures are plotted in the same graph for better comparison.

Temperature effect on SW
Spontaneous imbibition by seawater at 90°C and 110°C are presented in Figure 53 below.

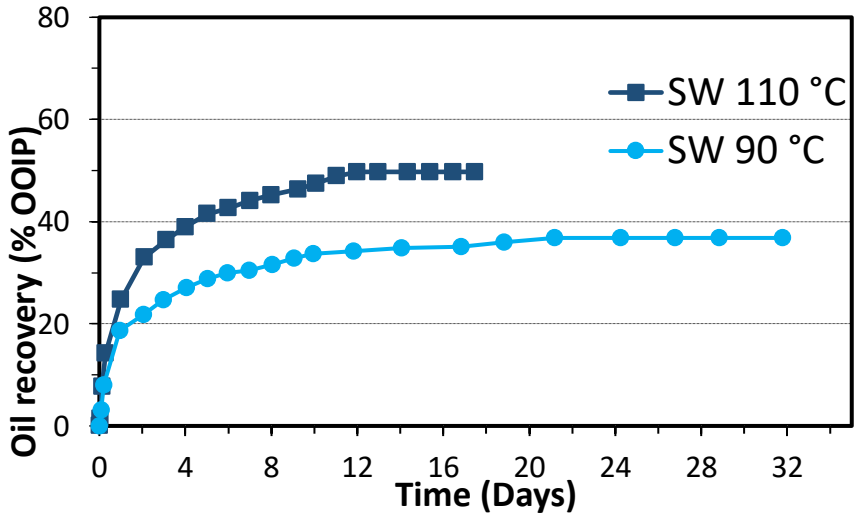

Figure 53: Oil recovery by spontaneous imbibition with SW. SK2 and SK6 chalk cores were used at 110°C and 90°C, respectively, with same initial saturation: S_{wi} =10% FW and S_{oi} = 90% oil with AN =0.58mgKOH/g.

Spontaneous imbibition with SW at 110° and 90°C resulted in 36.8% and 49.7% recovered oil, respectively. Hence, by only increasing the temperature with 20°C the oil recovery will improve by 12.9% OOIP. Since both SW brines contain the same concentration of the active ions that induces wettability alteration, the improvement of the oil recovery has to be temperature dependent. At 90°C the active ions are more hydrated and less reactive compared to the ions at 110°C. Water molecules start to break

around 100°C and the more the temperature increases the more the water molecules will break and the more reactive the potential determining ions become.

Temperature effect on DW-PS

At 90°C DW-PS reaches the plateau with 35.2% OOIP whereas at 110°C it reaches the plateau with 48.4% OOIP. With an increasement of 20°C the oil recovery increases with 13.2% OOIP. Same trend is observed as with SW in Figure 54. The active ions get less hydrated and more reactive at 110°C than at 90°C.

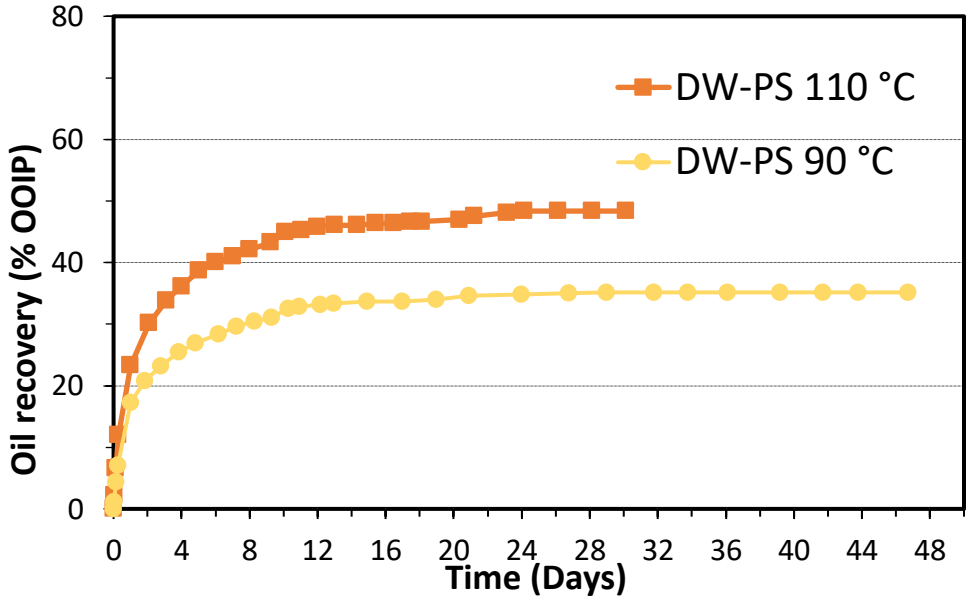

Figure 54: Spontaneous imbibition by DW-PS at 110°C and 90°C using SK3 and SK7, respectevly, with S_{wi} =10% FW and S_{oi} = 90% oil with AN =0.58mgKOH/g.

Temperature effect on SW-PS

44.8% of OOIP was recovered at 90°C with the brine SW-PS, see Figure 55. At 110°C the oil recovery did not reach the plateau due to precipitation that occurred in the inlet line of the spontaneous imbibition setup. The maximum reached recovery is 53.8% OOIP which gives the lowest improvement of oil recovery with only 9.0% OOIP compared to SW and DW-PS.

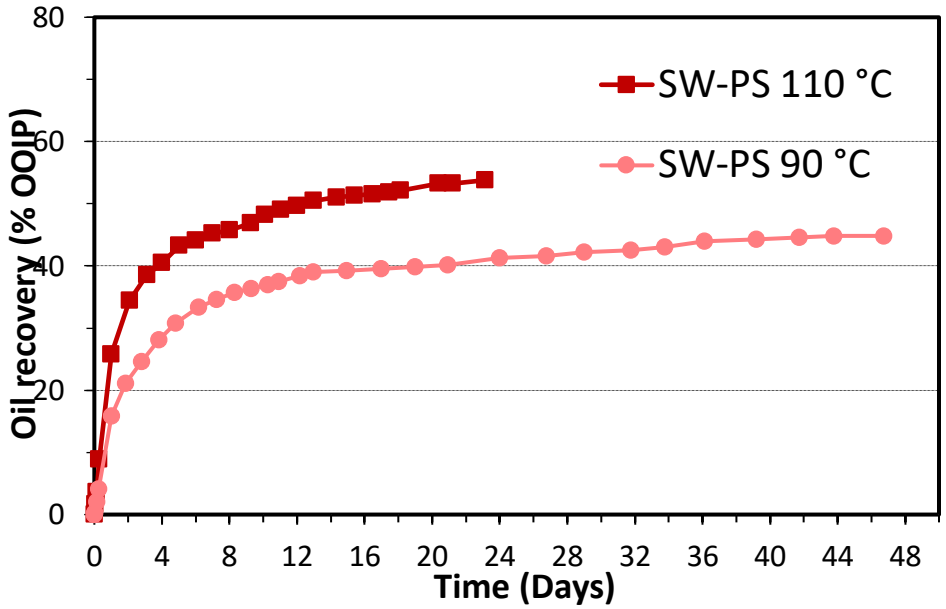

Figure 55: Spontaneous imbibition by SW-PS at 110°C and 90°C using SK4 and SK8, respectevly, with S_{wi} =10% FW and S_{oi} = 90% oil with AN =0.58mgKOH/g

From PHREEQC simulation, three minerals, anhydrite ($CaSO_4$) aragonite ($CaCO_3$) and calcite ($CaCO_3$), showed a relatively high potential of precipitating at 110°C. The ions that precipitated were most probably Ca^{2+} and SO_4^{2-}. No precipitation was detected in the imbibition cell nor at the outlet line. In a real-life situation the precipitation will probably not occur due to low temperature near the well bore. It may occur further to the reservoir and that is probably not a big issue. The OOIP% of each imbibition brine at 90°C and 110°C with the improved OOIP% are summarized in table 9 below.

Table 9: Summary of oil recovery where the increase of OOIP is related to temperature

Imbibition fluid	OOIP % T = 90°C	OOIP % T = 110°C	ΔOOIP %
SW	36.8	49.7	12.9
DW-PS	35.2	48.4	13.2
SW-PS	44.8	53.8	9.0

5.5.2. The Effect of Ion Composition

Since wettability alteration is driven by the three potential determining ions. It is of great importance to evaluate the effect of the ion composition in the brines. All the brines are presented below in figure 56.

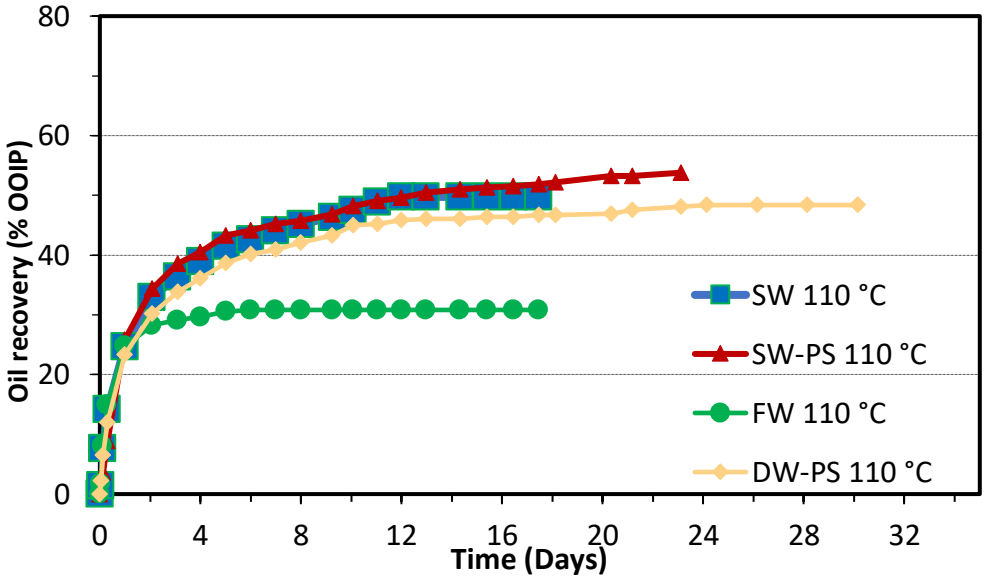

(a)

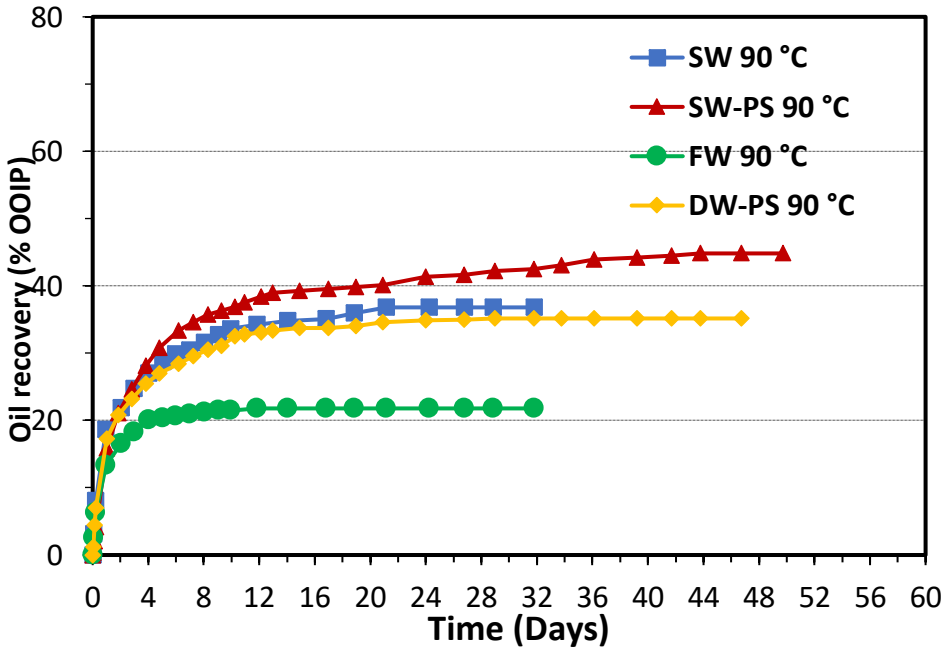

(b)

Figure 56: Spontaneous imbibition of FW, SW, DW-PS and SW-PS at (a) 110°C and (b) 90°C. All cores with S_{wi} =10% FW and S_{oi} = 90% oil with AN =0.58mgKOH/g

At 110°C and 90°C, SW, DW-PS and SW-PS alter the wettability of the chalk surface towards more water-wet conditions. All these three brines have higher imbibition rates than FW. Since FW do not contain SO_4^{2-} it is considered as the reference for wettability alteration. When comparing SW and SW-PS at 110°C there is clearly an overlap of the SI profiles. This overlap is not observed at 90°C meaning that the precipitated ions most probably are the active ions. The results of oil recovery are summarized in table 10 below. The maximum oil recovery obtained with the specific for each temperature is listed where ΔOOIP represents the increase in recovery compared to FW.

Table 10: Summary of oil recovery where the increase of OOIP is calculated from ionic point of view

Imbibition fluid	OOIP % T = 90°C	ΔOOIP %	OOIP % T = 110°C	ΔOOIP %
SW	36.8	15	49.7	21.2
DW-PS	35.2	13.4	48.4	17.6
SW-PS	44.8	23.0	53.8	23.0

6. Conclusion

Spontaneous imbibition by FW, SW, DW-PS and SW-PS at 90°C and 110°C was successfully performed on Stevns Klint chalk outcrop cores. The main conclusion are as follows:

- The use of PS salt in both SW and DW provided brines with Smart Water composition, holding adequate proportion of the three potential determining ions Mg^{2+}, Ca^{2+} and SO_4^{2-}.

- FW recovered 22% and 31% OOIP at 90 and 110 °C respectively, setting the base line for these system without having wettability alteration.

- DW-PS and SW-PS confirmed inducing wettability alteration as the %OOIP was significantly higher than imbibing FW with 35% and 45% recovered oil at 90°C and 48% and 54% recovered oil at 110 °C respectively, with an increase of 13.4% and 23.0% recovered oil at 90°C and 17% and 23.0% recovered oil at 110°C respectively, compared to FW.

- At 110°C SW-PS was not stable as it induced precipitation in the inlet line of the spontaneous imbibition set-up, SW-PS performance was closer to SW recovery with only 4 % higher difference in oil recovery.

- The performance of DW-PS at both 110°C and 90°C was slightly lower than SW with 1 to 2% difference in oil recovery. This provides an opportunity to obtain the same outstanding results on onshore fields where there is no or limited access to SW.

- The PHREEQC simulation showed consistency with the experimental results and stability of the composition.

7. Future Work

The results obtained by the experimental work in this thesis have the potential to be investigated further. The suggestions for future work are listed below:

- Reconfirm the experimental results by conducting the same tests at the same conditions. Focusing on precipitation and where it forms in the system, especially when using SW-PS brine.

- Perform spontaneous imbibition test with the same brines at lower temperatures to confirm/disconfirm wettability alteration of polysuphate brines.

- Optimize the mixing ratio of polysulphate salt with freshwater.

- Conduct chromatographic wettability test to quantify the chalks wetting state after spontaneous imbibition test.

- Evaluate the wettability effect of polysulphate in produced water.

References

Abdallah, W., J. S. Buckley, A. Carnegie, J. Edwards, B. Herold, E. Fordham, A. Graue, T. Habashy, N. Seleznev, C. Signer, H. Hussain, B. Montaron, and M. Ziauddin, 2007, Fundamentals of wettability: Oilfield Review, v. 19, p. 44-61.

Ahr, W. M., 2008, Geology of carbonate reservoirs: the identification, description, and characterization of hydrocarbon reservoirs in carbonate rocks: Hoboken, Hoboken: WILEY.

Akbar, M., B. Vissapragada, A. H. Alghamdi, D. Allen, M. Herron, A. Carnegie, D. Dutta, J. R. Olesen, R. D. Chourasiya, D. Logan, D. Stief, R. Netherwood, S. D. Russell, and K. Saxena, 2000, A Snapshot of Carbonate Reservoir Evaluation: Oilfield Review, v. 12, p. 20-41.

Al-Hadhrami, H. S., and M. J. Blunt, 2001, Thermally Induced Wettability Alteration To Improve Oil Recovery in Fractured Reservoirs: SPE Reservoir Evaluation & Engineering, v. 4, no. 03, p. 179-186, doi: 10.2118/71866-pa.

Alamooti, A. M., and F. K. Malekabadi, 2018, Fundamentals of Enhanced Oil and Gas Recovery from Conventional and Unconventional Reservoirs: ScienceDirect, ScienceDirect.

Amott, E., 1959, Observations Relating to the Wettability of Porous Rock: Transactions of the AIME, v. 216, no. 01, p. 156-162, doi: 10.2118/1167-g.

Anderson, W., 1986, Wettability Literature Survey- Part 2: Wettability Measurement: Journal of Petroleum Technology, v. 38, no. 11, p. 1246-1262, doi: 10.2118/13933-pa.

Arfken, G. B., D. F. Griffing, D. C. Kelly, and J. Priest, 1984, Chapter 16 - FLUID MECHANICS, *in* G. B. Arfken, D. F. Griffing, D. C. Kelly, and J. Priest, eds., International Edition University Physics, Academic Press, p. 306-325.

Atangana, A., 2018, Chapter 2 - Principle of Groundwater Flow, *in* A. Atangana, ed., Fractional Operators with Constant and Variable Order with Application to Geo-Hydrology, Academic Press, p. 15-47.

Austad, T., and J. Milter, 1997, Chemical flooding of oil reservoirs 6. Evaluation of the mechanism for oil expulsion by spontaneous imbibition of brine with and without surfactant in water-wet, low-permeable, chalk material: Colloids and surfaces. A, Physicochemical and engineering aspects, v. 113, no. 3, p. 269-278, doi: 10.1016/0927-7757(96)03631-X.

Austad, T., S. Strand, M. V. Madland, T. Puntervold, and R. I. Korsnes, 2007, Seawater in Chalk: An EOR and Compaction Fluid: International Petroleum Technology Conference.

Austad, T., S. Strand, M. V. Madland, T. Puntervold, and R. I. Korsnes, 2008, Seawater in Chalk: An EOR and Compaction Fluid: SPE Reservoir Evaluation & Engineering, v. 11, no. 04, p. 648-654, doi: 10.2118/118431-pa.

Austad, T., S. Strand, and T. Puntervold, 2009, IS WETTABILITY ALTERATION OF CARBONATES BY SEAWATER CAUSED BY ROCK DISSOLUTION?

Ayirala, S., and A. Yousef, 2014, Optimization Study of a Novel Water-Ionic Technology for Smart-Waterflooding Application in Carbonate Reservoirs: Oil and gas facilities, v. 3, no. 5, p. 072-082, doi: 10.2118/169052-PA.

Bissell, H. J., and G. V. Chilingar, 1967, Chapter 4 Classification of Sedimentary Carbonate Rocks, *in* G. V. Chilingar, H. J. Bissell, and R. W. Fairbridge, eds., Developments in Sedimentology9, Elsevier, p. 87-168.

Bjørlykke, K., 2015, Petroleum Geoscience : From Sedimentary Environments to Rock Physics, Berlin, Heidelberg, Springer Berlin Heidelberg : Imprint: Springer.

Burton, G., 2000, Chemical Ideas, Pearson Education.
Cheryan, M., 1998, Ultrafiltration and microfiltration handbook, 2nd ed. ed., v.: Lancaster, Pa, Technomic Publ.
Craig, F. F., 1971, The reservoir engineering aspects of waterflooding: Henry L. Doherty seriesvol. 3: New York, Henry L. Doherty Memorial Fund of AIME.
Cuiec, L., 1984, Rock/Crude-Oil Interactions and Wettability: An Attempt To Understand Their Interrelation: SPE Annual Technical Conference and Exhibition.
Donaldson, E. C., and W. Alam, 2008, Wettability: Austin, Austin: Gulf Publishing Company.
Donaldson, E. C., R. D. Thomas, and P. B. Lorenz, 1969, Wettability Determination and Its Effect on Recovery Efficiency: Society of Petroleum Engineers Journal, v. 9, no. 01, p. 13-20, doi: 10.2118/2338-pa.
Dubey, S. T., and P. H. Doe, 1993, Base Number and Wetting Properties of Crude Oils: SPE Reservoir Engineering, v. 8, no. 03, p. 195-200, doi: 10.2118/22598-pa.
Fan, T., and J. S. Buckley, 2007, Acid Number Measurements Revisited: SPE Journal, v. 12, no. 04, p. 496-500, doi: 10.2118/99884-pa.
Fathi, J., 2012, Water–Based Enhanced Oil Recovery (EOR) in Carbonate Reservoirs
Initial Wetting Condition and Wettability Alteration by “Smart Water”.
Fathi, S. J., T. Austad, and S. Strand, 2011, Water-Based Enhanced Oil Recovery (EOR) by “Smart Water”: Optimal Ionic Composition for EOR in Carbonates: Energy & Fuels, v. 25, no. 11, p. 5173-5179, doi: 10.1021/ef201019k.
Frykman, P., 2001, Spatial variability in petrophysical properties in Upper Maastrichtian chalk outcrops at Stevns Klint, Denmark, v. 18, no. 10, p. 1041-1062.
Ghedan, S., C. H. Canbaz, D. Boyd, G. M. Corelab, and M. Haggag, 2010, Wettability Profile of a Thick Carbonate Reservoir by the New Rise in Core Wettability Characterization Method: Abu Dhabi International Petroleum Exhibition and Conference.
Green, D. W., and G. P. Willhite, 2018, Enhanced Oil Recovery, SPE, 912 p, p. 1.
Hall, H. N., 1961, Analysis of Gravity Drainage: Journal of Petroleum Technology, v. 13, no. 09, p. 927-936, doi: 10.2118/1517-g-pa.
Hognesen, E. J., S. Strand, and T. Austad, 2005, Waterflooding of preferential oil-wet carbonates: Oil recovery related to reservoir temperature and brine composition: SPE Europec/EAGE Annual Conference.
ICL, 2022a, Information Provided by the Company
ICL, 2022b, Polysulphate is a new fertilizer, high in sulphate, available in its natural state, and mined in the UK. Web. Accessed, https://polysulphate.com/global-en/introducing-polysulphate/.
Lucia, F. J., 2007, Carbonate reservoir characterization : an integrated approach, 2nd ed. ed., v.: Berlin, Springer.
Luyk, E., 2019, Sputter Coating for SEM: How This Sample Preparation Technique Assists Your Imaging. Web. Accessed, https://www.thermofisher.com/blog/microscopy/sputter-coating-for-sem-how-this-sample-preparation-technique-assists-your-imaging/.
McPhee, C., J. Reed, and I. Zubizarreta, 2015, Chapter 7 - Wettability and Wettability Tests, *in* C. McPhee, J. Reed, and I. Zubizarreta, eds., Developments in Petroleum Science64, Elsevier, p. 313-345.
Morrow, N. R., 1979, Interplay of Capillary, Viscous And Buoyancy Forces In the Mobilization of Residual Oil: Journal of Canadian Petroleum Technology, v. 18, no. 03, doi: 10.2118/79-03-03.
Morrow, N. R., 1990, Wettability and Its Effect on Oil Recovery: Journal of Petroleum Technology, v. 42, no. 12, p. 1476-1484, doi: 10.2118/21621-pa.

Morrow, N. R., and G. Mason, 2001, Recovery of oil by spontaneous imbibition: Current Opinion in Colloid & Interface Science, v. 6, no. 4, p. 321-337, doi: https://doi.org/10.1016/S1359-0294(01)00100-5.
Pierre, A., J. M. Lamarche, R. Mercier, A. Foissy, and J. Persello, 1990, CALCIUM AS POTENTIAL DETERMINING ION IN AQUEOUS CALCITE SUSPENSIONS: Journal of Dispersion Science and Technology, v. 11, no. 6, p. 611-635, doi: 10.1080/01932699008943286.
Piñerez, I., T. Puntervold, S. Strand, P. Hopkins, P. Aslanidis, H. S. Yang, and M. S. Kinn, 2020, Core wettability reproduction: A new solvent cleaning and core restoration strategy for chalk cores: Journal of Petroleum Science and Engineering, v. 195, p. 107654, doi: https://doi.org/10.1016/j.petrol.2020.107654.
Puntervold, T., 2008, Waterflooding of carbonate reservoirs : EOR by wettability alteration: Doctoral thesis thesis, University of Stavanger, uis.brage.unit.no.
Puntervold, T., S. Strand, and T. Austad, 2007, New Method To Prepare Outcrop Chalk Cores for Wettability and Oil Recovery Studies at Low Initial Water Saturation: Energy & Fuels, v. 21, no. 6, p. 3425-3430, doi: 10.1021/ef700323c.
Puntervold, T., S. Strand, and T. Austad, 2009, Coinjection of Seawater and Produced Water to Improve Oil Recovery from Fractured North Sea Chalk Oil Reservoirs: Energy Fuels, v. 23, no. 5, p. 2527-2536, doi: 10.1021/ef801023u.
Puntervold, T., S. Strand, R. Ellouz, and T. Austad, 2015, Modified seawater as a smart EOR fluid in chalk: Journal of Petroleum Science and Engineering, v. 133, p. 440-443, doi: https://doi.org/10.1016/j.petrol.2015.06.034.
Schlumberger, Carbonate Reservoirs Overcome Challenging Heterogeneity. Schlumberger. Web. Accessed: 01.05.22, https://www.slb.com/technical-challenges/carbonates.
Schlumberger, Permeability.
Shariatpanahi, S. F., P. Hopkins, H. Aksulu, S. Strand, T. Puntervold, and T. Austad, 2016, Water Based EOR by Wettability Alteration in Dolomite: Energy & Fuels, v. 30, no. 1, p. 180-187, doi: 10.1021/acs.energyfuels.5b02239.
Standnes, D. C., and T. Austad, 2000, Wettability alteration in chalk: 1. Preparation of core material and oil properties: Journal of Petroleum Science and Engineering, v. 28, no. 3, p. 111-121, doi: https://doi.org/10.1016/S0920-4105(00)00083-8.
Strand, S., E. J. Høgnesen, and T. Austad, 2006a, Wettability alteration of carbonates—Effects of potential determining ions (Ca2+ and SO42−) and temperature: Colloids and Surfaces A: Physicochemical and Engineering Aspects, v. 275, no. 1, p. 1-10, doi: https://doi.org/10.1016/j.colsurfa.2005.10.061.
Strand, S., T. Puntervold, and T. Austad, 2008, Effect of Temperature on Enhanced Oil Recovery from Mixed-Wet Chalk Cores by Spontaneous Imbibition and Forced Displacement Using Seawater: Energy & Fuels, v. 22, no. 5, p. 3222-3225, doi: 10.1021/ef800244v.
Strand, S., D. C. Standnes, and T. Austad, 2006b, New wettability test for chalk based on chromatographic separation of SCN− and SO42−: Journal of Petroleum Science and Engineering, v. 52, no. 1, p. 187-197, doi: https://doi.org/10.1016/j.petrol.2006.03.021.
Wilson, J. L., 1975, Principles of Carbonate Sedimentation, *in* J. L. Wilson, ed., Carbonate Facies in Geologic History: New York, NY, Springer New York, p. 1-19.
Zhang, P., 2006, Water-based EOR in Fractured Chalk – Wettability and Chemical Additives Phd thesis.
Zhang, P., and T. Austad, 2005, The Relative Effects of Acid Number and Temperature on Chalk Wettability: SPE International Symposium on Oilfield Chemistry.

Zhang, P., and T. Austad, 2006, Wettability and oil recovery from carbonates: Effects of temperature and potential determining ions: Colloids and Surfaces A: Physicochemical and Engineering Aspects, v. 279, no. 1, p. 179-187, doi: https://doi.org/10.1016/j.colsurfa.2006.01.009.

Zhang, P., M. T. Tweheyo, and T. Austad, 2007, Wettability Alteration and Improved Oil Recovery in Chalk: The Effect of Calcium in the Presence of Sulfate: Energy Fuels, v. 20, no. 5, p. 2056-2062, doi: 10.1021/ef0600816.

Appendix

Imbibition data

Imbibition data for SK1 with FW at 110°C

Time (days)	Recovery (ml)	Recovery % OOIP)
0.0	0.0	0.0
0.0	0.6	1.7
0.1	2.8	8.1
0.3	5.2	15.0
1.0	8.6	24.8
2.0833	9.8	28.2
3.1	10.1	29.1
4.0	10.3	29.7
5.0	10.6	30.5
6.0	10.7	30.8
7.0	10.7	30.8
8.0	10.7	30.8
9.3	10.7	30.8
10.1	10.7	30.8
11.0	10.7	30.8
12.0	10.7	30.8
13.0	10.7	30.8
14.3	10.7	30.8
15.4	10.7	30.8
16.5	10.7	30.8
17.5	10.7	30.8

Imbibition data for SK2 with SW at 110°C

Time (days)	Recovery (ml)	Recovery % OOIP)
0.0	0.0	0.0
0.0	0.5	1.4
0.1	2.7	7.7
0.3	5.0	14.2
1.0	8.7	24.7
2.0833	11.6	33.0
3.1	12.8	36.4
4.0	13.7	38.9
5.0	14.6	41.5
6.0	15.0	42.6
7.0	15.5	44.1
8.0	15.9	45.2
9.3	16.3	46.3
10.1	16.7	47.5
11.0	17.2	48.9
12.0	17.5	49.7
13.0	17.5	49.7
14.3	17.5	49.7
15.4	17.5	49.7
16.5	17.5	49.7
17.5	17.5	49.7

Imbibition data for SK3 with DW-PS at 110°C

Time (days)	Recovery (ml)	Recovery % OOIP)
0.0	0.0	0.0
0.0	0.8	2.3
0.1	2.3	6.5
0.3	4.2	12.0
1.0	8.2	23.3
2.0833	10.6	30.2
3.1	11.9	33.9
4.0	12.7	36.1
5.0	13.6	38.7
6.0	14.1	40.1
7.0	14.4	41.0
8.0	14.8	42.1
9.3	15.2	43.2
10.1	15.8	45.0
11.0	15.9	45.2
12.0	16.1	45.8
13.0	16.2	46.1
14.3	16.2	46.1
15.4	16.3	46.4
16.5	16.3	46.4
17.5	16.4	46.7
18.1	16.4	46.7
20.4	16.5	46.9
21.2	16.7	47.5
23.1	16.9	48.1
24.1	17.0	48.4
26.1	17.0	48.4
28.1	17.0	48.4
30.1	17.0	48.4

Imbibition data for SK4 with SW-PS at 110°C

Time (days)	Recovery (ml)	Recovery % OOIP)
0.0	0.0	0.0
0.0	0.6	1.7
0.1	1.3	3.6
0.3	3.2	8.9
1.0	9.3	25.8
2.0833	12.4	34.4
3.1	13.9	38.5
4.0	14.6	40.5
5.0	15.6	43.3
6.0	15.9	44.1
7.0	16.3	45.2
8.0	16.5	45.8
9.3	16.9	46.9
10.1	17.4	48.2
11.0	17.7	49.1
12.0	17.9	49.6
13.0	18.2	50.5
14.3	18.4	51.0
15.4	18.5	51.3
16.5	18.6	51.6
17.5	18.7	51.9
18.1	18.8	52.1
20.4	19.2	53.2
21.2	19.2	53.2
23.1	19.4	53.8

Imbibition data for SK5 with FW at 90°C

Time (days)	Recovery (ml)	Recovery % OOIP)
0.0	0.0	0.0
0.1	0.9	2.6
0.2	2.2	6.2
1.0	4.6	13.4
2.0	5.7	16.6
3.0	6.3	18.3
4.0	6.9	20.0
5.0	7.0	20.3
6.0	7.1	20.6
7.0	7.2	20.9
8.0	7.3	21.2
9.0	7.4	21.5
10.0	7.4	21.5
11.8	7.5	21.8
14.0	7.5	21.8
16.8	7.5	21.8
18.8	7.5	21.8
21.2	7.5	21.8
24.3	7.5	21.8
26.8	7.5	21.8
28.8	7.5	21.8
31.8	7.5	21.8

Imbibition data for SK6 with SW at 90°C

Time (days)	Recovery (ml)	Recovery % OOIP)
0.0	0.0	0.0
0.1	1.1	3.2
0.2	2.8	8.1
1.0	6.5	18.7
2.0	7.6	21.9
3.0	8.6	24.7
4.0	9.4	27.0
5.0	10.0	28.8
6.0	10.4	29.9
7.0	10.6	30.5
8.0	11.0	31.6
9.0	11.4	32.8
10.0	11.7	33.6
11.8	11.9	34.2
14.0	12.1	34.8
16.8	12.2	35.1
18.8	12.5	35.9
21.2	12.8	36.8
24.3	12.8	36.8
26.8	12.8	36.8
28.8	12.8	36.8
31.8	12.8	36.8

Imbibition data for SK7 with DW-PS at 90°C

Time (days)	Recovery (ml)	Recovery % OOIP)
0.0	0.0	0.0
0.0	0.4	1.2
0.1	1.5	4.4
0.3	2.4	7.0
1.0	5.9	17.3
1.8333	7.1	20.8
2.8	7.9	23.1
3.8	8.7	25.5
4.8	9.2	27.0
6.2	9.7	28.4
7.2	10.1	29.6
8.3	10.4	30.5
9.3	10.6	31.1
10.3	11.1	32.5
10.9	11.2	32.8
12.1	11.3	33.1
13.0	11.4	33.4
14.9	11.5	33.7
17.0	11.5	33.7
19.0	11.6	34.0
20.9	11.8	34.6
24.0	11.9	34.9
26.8	12.0	35.0
29.0	12.0	35.2
31.8	12.0	35.2
33.8	12.0	35.2
36.1	12.0	35.2
39.2	12.0	35.2
41.7	12.0	35.2
43.8	12.0	35.2
46.7	12.0	35.2

Imbibition data for SK8 with SW-PS at 90°C

Time (days)	Recovery (ml)	Recovery % OOIP)
0.0	0.0	0.0
0.0	0.1	0.3
0.1	0.7	2.1
0.3	1.4	4.1
1.0	5.4	15.8
1.8333	7.2	21.1
2.8	8.4	24.6
3.8	9.6	28.1
4.8	10.5	30.8
6.2	11.4	33.4
7.2	11.8	34.6
8.3	12.2	35.7
9.3	12.4	36.3
10.3	12.6	36.9
10.9	12.8	37.5
12.1	13.1	38.4
13.0	13.3	39.0
14.9	13.4	39.3
17.0	13.5	39.6
19.0	13.6	39.8
20.9	13.7	40.1
24.0	14.1	41.3
26.8	14.2	41.6
29.0	14.4	42.2
31.8	14.5	42.5
33.8	14.7	43.1
36.1	15.0	44.0
39.2	15.1	44.2
41.7	15.2	44.5
43.8	15.3	44.8
46.7	15.3	44.8
49.7	15.3	44.8

Ion chromatography results

	Chloride (Mm)	Sulphate (Mm)	Sodium (Mm)	potassium (Mm)	Magnesium (Mm)	Calcium (Mm)
DW	1.2	0.1	0.0	0.0	0.0	0.0
DW-PS	9.2	31.5	6.3	17.4	5.8	15.2
SW	525.0	24.0	450.0	10.0	45.0	13.0
SW-PS	528.5	55.9	466.2	28.2	47.9	29.6